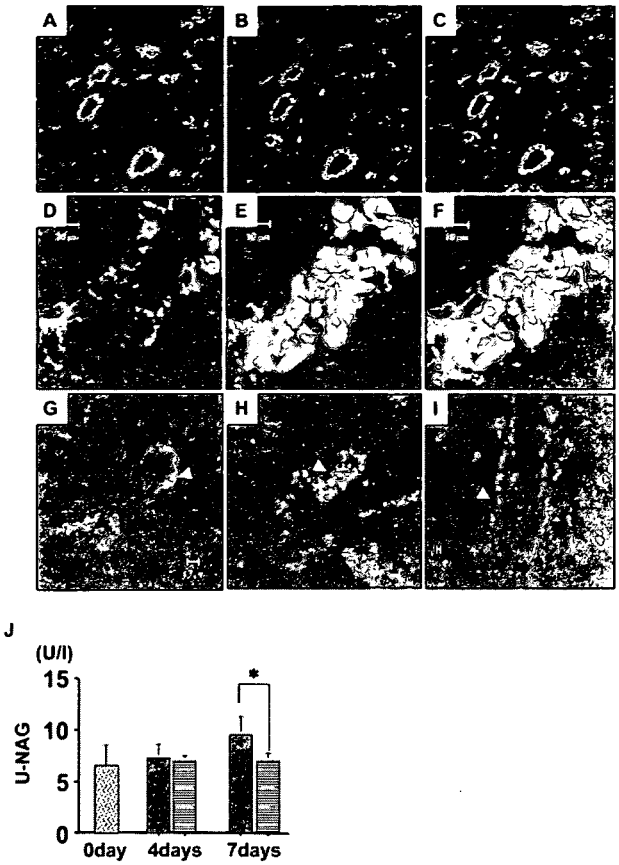


**Figure 8.** Engraftment of rKS56 cells to injured tubules in renal ischemia-reperfusion model. *A–C)* Double staining of Di-O-labeled rKS56 cells (green) and cytokeratin (red) using kidney sections obtained from rats with renal ischemia-reperfusion and treated with transplantation of rKS56 cells. Representative fluorescent photomicrographs of corticomedullary junction lesion of left kidneys 7 days after cell transplantation are shown. rKS56 cells (green) were incorporated into tubules at corticomedullary junction, and portions of cytokeratin positive cells (red, *A*) were rKS56 cells (green, *B*) as confirmed on the merged image (*C*). *D–F)* Double staining of Di-O-labeled rKs56 cells (green) and AQP-1 (red) using kidney sections obtained from rats with renal ischemia-reperfusion and treated with transplantation of rKS56 cells (day 7). Portions of AQP-1 positive cells (red, *D*) were rKS56 cells (green, *E*) as confirmed on the merged image (F). Di-O positive (rKS56) cells were observed partly in subcortical area (*G*) and medulla (*I*), but mostly in corticomedullary junction lesion (*H*). Implantation of rKS56 cells suppressed U-NAG levels 7 days after I/R (*J*). 0 day: 0 day for control, 4 days: 4 days after I/R, 7 days: 7 days after I/R. Dotted bar: 0 day group, filled bar: vehicle control I/R group, hatched bar: rKS56 cells-implanted group after I/R. $*P < 0.05$ vs. vehicle control I/R group. Each column consists of means ± SE.

necrosis model using rKS56 cells. Since rKS56 cells migrated, attached and differentiated to mainly tubulointerstitial cells, rKS56 cells implantation might have resulted in the suppression of U-NAG elevation in I/R model. It is possible that direct intrarenal injection of rKS56 cells might have resulted in slightly increased s-Cr and BUN values, and subsequent analysis using various distinct ways of delivery of rKS56 cells such as intravenous, intra-arterial or retrograde ureteral approaches are underway to determine the optimal approach for rKS56 cell therapy.

Oliver et al. reported that renal papilla is a niche for adult kidney stem cells (41). They proved slow cell cycling cells location by BrdU-retaining in embryo kidney. rKS56 cells are harvested from S3 segments, and grew exponentially. So, rKS56 cells might have a progenitor character rather than stem cell character. Stem cell in papilla may migrate to corticomedullary junction, differentiate to progenitor cells and contribute to cell turnover and regeneration.

In conclusion, we were able to isolate renal highly proliferative cells from the S3 segment of proximal tubule in adult rat kidney. The rKS56 cells exhibited self-renewal and multipotency restricted to renal cells in vitro and in vivo. However, the karyotype of rKS56 cells were nearly triploid, suggesting that rKS56 cell is a cell line with triploidy holding highly proliferative potential and possibly having capacity to serve as renal stem/progenitor cells. In this regard, rKS56 cell might not be defined as a physiological renal tissue stem/progenitor cell. Establishment of rKS56 cells will facilitate investigating other characteristics of adult renal stem cells and the regulatory mechanisms of phenotype, which may contribute to the future development of cytotherapy for regeneration of injured kidney. The use of adult tissue stem cells would be advantageous over embryonic tissue stem cells by virtue of the limited source of human embryonic kidneys and the circumvention of ethical issues involving embryos. FJ

A portion of this study was supported by the Health and Labour Sciences Research Grants for Research on Human Genome, Tissue Engineering Food Biotechnology from the Ministry of Health Labour and Welfare of Japan (to H.M.). We are grateful to Dr. H. Nonoguchi (Kumamoto University, Japan) for technical assistance in performing microdissection of nephron segments. We would like to thank Dr. M. Yasui (Johns Hopkins University School of Medicine) for helpful comments on the manuscript.

## REFERENCES

1. Rietze, R. L., Valcanis, H., Brooker, G. F., Thomas, T., Voss, A. K., and Bartlett, P. F. (2001) Purification of a pluripotent neural stem cell from the adult mouse brain. *Nature (London)* **412,** 736–739
2. Gussoni, E., Soneoka, Y., Strickland, C. D., Buzney, E. A., Khan, M. K., Flint, A. F., Kunkel, L. M., and Mulligan, R. C. (1999) Dystrophin expression in the mdx mouse restored by stem cell transplantation. *Nature (London)* **401,** 390–394
3. Kocher, A. A., Schuster, M. D., Szabolcs, M. J., Takuma, S., Burkhoff, D., Wang, J., Homma, S., Edwards, N. M., and Itescu, S. (2001) Neovascularization of ischemic myocardium by human bone-marrow-derived angioblasts prevents cardiomyocyte apoptosis, reduces remodeling and improves cardiac function. *Nat. Med.* **7,** 430–436
4. Weissman, I. L. (2000) Stem cells: units of development, units of regeneration, and units in evolution. *Cell* **100,** 157–168
5. Orlic, D., Kajstura, J., Chimenti, S., Bodine, D. M., Leri, A., and Anversa, P. (2001) Bone marrow stem cells regenerate infarcted myocardium. *Nature (London)* **410,** 701–704
6. Fuchs, E., and Segre, J. A. (2000) Stem cells: a new lease on life. *Cell* **100,** 143–155

7. Asahara, T., Murohara, T., Sullivan, A., Silver, M., van der Zee, R., Li, T., Witzenbichler, B., Schatteman, G., and Isner, J. M. (1997) Isolation of putative progenitor endothelial cells for angiogenesis. *Science* **275,** 964–967
8. Ferrari, G., Cusella-De Angelis, G., Coletta, M., Paolucci, E., Stornaiuolo, A., Cossu, G., and Mavilio, F. (1998) Muscle regeneration by bone marrow-derived myogenic progenitors. *Science* **279,** 1528–1530
9. Jiang, Y., Jahagirdar, B. N., Reinhardt, R. L., Schwartz, R. E., Keene, C. D., Ortiz-Gonzalez, X. R., Reyes, M., Lenvik, T., Lund, T., Blackstad, M., et al. (2002) Pluripotency of mesenchymal stem cells derived from adult marrow. *Nature (London)* **418,** 41–49
10. Schwartz, R. E., Reyes, M., Koodie, L., Jiang, Y., Blackstad, M., Lund, T., Lenvik, T., Johnson, S., Hu, W. S., and Verfaillie, C. M. (2002) Multipotent adult progenitor cells from bone marrow differentiate into functional hepatocyte-like cells. *J. Clin. Invest.* **109,** 1291–1302
11. Okamoto, R., Yajima, T., Yamazaki, M., Kanai, T., Mukai, M., Okamoto, S., Ikeda, Y., Hibi, T., Inazawa, J., and Watanabe, M. (2002) Damaged epithelia regenerated by bone marrow-derived cells in the human gastrointestinal tract. *Nat. Med.* **8,** 1011–1017
12. Eglitis, M. A., and Mezey, E. (1997) Hematopoietic cells differentiate into both microglia and macroglia in the brains of adult mice. *Proc. Natl. Acad. Sci. USA* **94,** 4080–4085
13. Ito, T., Suzuki, A., Imai, E., Okabe, M., and Hori, M. (2001) Bone marrow is a reservoir of repopulating mesangial cells during glomerular remodeling. *J. Am. Soc. Nephrol.* **12,** 2625–2635
14. Cornacchia, F., Fornoni, A., Plati, A. R., Thomas, A., Wang, Y., Inverardi, L., Striker, L. J., and Striker, G. E. (2001) Glomerulosclerosis is transmitted by bone marrow-derived mesangial cell progenitors. *J. Clin. Invest.* **108,** 1649–1656
15. Tateishi-Yuyama, E., Matsubara, H., Murohara, T., Ikeda, U., Shintani, S., Masaki, H., Amano, K., Kishimoto, Y., Yoshimoto, K., Akashi, H., et al. (2002) Therapeutic Angiogenesis using Cell Transplantation (TACT) Study Investigators: Therapeutic angiogenesis for patients with limb ischaemia by autologous transplantation of bone-marrow cells: a pilot study and a randomised controlled trial. *Lancet* **360,** 427–435
16. Nath, K. A. (1992) Tubulointerstitial changes as a major determinant in the progression of renal damage. *Am. J. Kidney Dis.* **20,** 1–17
17. Makino, H., Kashihara, N., Sugiyama, H., Kanao, K., Sekikawa, T., Okamoto, K., Maeshima, Y., Ota, Z., and Nagai, R. (1996) Phenotypic modulation of the mesangium reflected by contractile proteins in diabetes. *Diabetes* **45,** 488–495
18. Maeshima, Y., Kashihara, N., Yasuda, T., Sugiyama, H., Sekikawa, T., Okamoto, K., Kanao, K., Watanabe, Y., Kanwar, Y. S., and Makino, H. (1998) Inhibition of mesangial cell proliferation by E2F decoy oligodeoxynucleotide in vitro and in vivo. *J. Clin. Invest.* **101,** 2589–2597
19. Oliver, J. A., Barasch, J., Yang, J., Herzlinger, D., and Al-Awqati, Q. (2002) Metanephric mesenchyme contains embryonic renal stem cells. *Am. J. Physiol.* **283,** F799–F809
20. Dekel, B., Burakova, T., Arditti, F. D., Reich-Zeliger, S., Milstein, O., Aviel-Ronen, S., Rechavi, G., Friedman, N., Kaminski, N., Passwell, J. H., et al. (2003) Human and porcine early kidney precursors as a new source for transplantation. *Nat. Med.* **9,** 53–60
21. Reynolds, B. A., and Weiss, S. (1996) Clonal and population analysis demonstrate that an EGF-responsive mammalian embryonic CNS precursor is a stem cell. *Dev. Biol.* **175,** 1–13
22. Cha, J. H., Kim, Y. H., Jung, J. Y., Han, K. H., Madsen, K. M., and Kim, J. (2001) Cell proliferation in the loop of Henley in the developing rat kidney. *J. Am. Soc. Nephrol.* **12,** 1410–1421
23. Disashi, T., Nonoguchi, H., Iwaoka, T., Naomi, S., Nakayama, Y., Shimada, K., Tanzawa, K., and Tomita, K. (1997) Endothelin converting enzyme-1 gene expression in the kidney of spontaneously hypertensive rats. *Hypertension* **30,** 1591–1597
24. Maeshima, Y., Sudhakar, A., Lively, J. C., Ueki, K., Kharbanda, S., Kahn, C. R., Sonenberg, N., Hynes, R. O., and Kalluri, R. (2002) Tumstatin, an endothelial cell-specific inhibitor of protein synthesis. *Science* **295,** 140–143
25. Sherley, J. L. (2002) Asymmetric cell kinetics genes: the key to expansion of adult stem cells in culture. *Sci. World J.* **2,** 1906–1921
26. Uchida, N., Buck, D. W., He, D., Reitsma, M. J., Masek, M., Phan, T. V., Tsukamoto, A. S., Gage, F. H., and Weissman, I. L. (2000) Direct isolation of human central nervous system stem cells. *Proc. Natl. Acad. Sci. USA* **97,** 14720–14725
27. Taniguchi, H., Toyoshima, T., Fukao, K., and Nakauchi, H. (1996) Presence of hematopoietic stem cells in the adult liver. *Nat. Med.* **2,** 198–203
28. Nakauchi, H. (2004) Isolation and clonal characterization of hematopoietic and liver stem cells. *Cornea* **23,** S2–S7
29. Valerius, M. T., Patterson, L. T., Feng, Y., and Potter, S. S. (2002) Hoxa 11 is upstream of Integrin a8 expression in the developing kidney. *Proc. Natl. Acad. Sci. USA* **99,** 8090–8095
30. Imgrund, M., Grone, E., Grone, H. J., Kretzler, M., Holzman, L., Schlondorff, D., and Rothenpieler, U. W. (1999) Re-expression of the developmental gene Pax-2 during experimental acute tubular necrosis in mice 1. *Kidney Int.* **56,** 1423–1431
31. Lavker, R. M., and Sun, T. T. (2000) Epidermal stem cells: Properties, markers and location. *Proc. Natl. Acad. Sci. USA* **97,** 13473–13475
32. Nakamura, M., Okano, H., Blendy, J. A., and Montell, C. (1994) Musashi, a neural RNA-binding protein required for *Drosophila* adult external sensory organ development. *Neuron* **13,** 67–81
33. Potten, C. S., Booth, C., Tudor, G. L., Booth, D., Brady, G., Hurley, P., Ashton, G., Clarke, R., Sakakibara, S., and Okano, H. (2003) Identification of a putative intestinal stem cell and early lineage marker; musashi-1. *Differentiation* **71,** 28–41
34. Kayahara, T., Sawada, M., Takaishi, S., Fukui, H., Seno, H., Fukuzawa, H., Suzuki, K., Hiai, H., Kageyama, R., Okano, H., et al. (2003) Candidate markers for stem and early progenitor cells, Musashi-1 and Hes1, are expressed in crypt base columnar cells of mouse small intestine. *FEBS Lett.* **535,** 131–135
35. Clarke, R. B., Anderson, E., Howell, A., and Potton, C. S. (2003) Regulation of human breast epithelial stem cells. *Cell Prolif.* **36, Suppl. 1,** 45–58
36. Al-Awqati, Q., and Oliver, J. A. (2002) Stem cells in the kidney. *Kidney Int.* **61,** 387–395
37. Alison, M. R., Poulsom, R., Jeffery, R., Dhillon, A. P., Quaglia, A., Jacob, J., Novelli, M., Prentice, G., Williamson, J., and Wright, N. A. (2000) Hepatocytes from non-hepatic adult stem cells. *Nature (London)* **406,** 257
38. Poulsom, R., Forbes, S. J., Hodivala-Dilke, K., Ryan, E., Wyles, S., Navaratnarasah, S., Jeffery, R., Hunt, T., Alison, M., Cook, T., et al. (2001) Bone marrow contributes to renal parenchymal turnover and regeneration. *J. Pathol.* **195,** 229–235
39. Lin, F., Cordes, K., Li, L., Hood, L., Couser, W. G., Shankland, S. J., and Igarashi, P. (2003) Hematopoietic stem cells contribute to the regeneration of renal tubules after ischemia-reperfusion injury in mice. *J. Am. Soc. Nephrol.* **14,** 1188–1199
40. Kale, S., Karihaloo, A., Clark, P. R., Kashgarian, M., Krause, D. S., and Cantley, L. G. (2003) Bone marrow stem cells contribute to repair of the ischemically injured renal tubule. *J. Clin. Invest.* **112,** 42–49
41. Oliver, J. A., Maarouf, O., Cheema, F. H., Martens, T. P., and Al-Awqati, Q. (2004) The renal papilla is a niche for adult kidney stem cells. *J. Clin. Invest.* **114,** 795–804

*Received for publication March 2, 2005.*
*Accepted for publication June 27, 2005.*

Original Paper

nephron
Experimental
Nephrology

Nephron Exp Nephrol 2006;104:e6–e14
DOI: 10.1159/000093258

Received: November 21, 2005
Accepted: January 30, 2006
Published online: May 11, 2006

# Efficacy of Darbepoetin in Doxorubicin-Induced Cardiorenal Injury in Rats

Eisei Noiri[a, c, d] Nobuo Nagano[e] Kosuke Negishi[a] Kent Doi[a] Sonoe Miyata[e]
Megumi Abe[e] Tamami Tanaka[a] Koji Okamoto[a] Norio Hanafusa[c]
Yasushi Kondo[c] Nobukazu Ishizaka[b] Toshiro Fujita[a, c]

Departments of [a]Nephrology and Endocrinology and [b]Cardiovascular Medicine and [c]Center for Dialysis, Apheresis, and Applied Medicine, University Hospital, and [d]Center for NanoBio Integration, University of Tokyo, Tokyo, and [e]Pharmaceutical Development Laboratories, Kirin Brewery Co., Ltd., Takasaki, Japan

**Key Words**
Darbepoetin · Doxorubicin-induced cardiorenal injury · Rat model, cardiorenal injury

**Abstract**
This study was intended to elucidate the efficacy of an erythropoietin analog in cardiorenal dysfunction syndrome using a rodent model. Cardiorenal dysfunction was induced using doxorubicin hydrochloride (DXR). Lower doses (3 μg/kg) and higher doses (30 μg/kg) of darbepoetin alfa (DA) were used for intervention. Blood examinations for creatinine, blood urea nitrogen, iron, and hemoglobin were performed until 11 weeks after starting DA administration. Urine collection was performed 10 weeks after starting DA, and protein, iron, and N-acetyl-β-*D*-glucosaminidase levels and antioxidation capacity of DA were determined. The dry left ventricular heart weight was measured, when the animals were sacrificed 11 weeks after starting DA administration. Histological analyses were performed for interstitial fibrotic changes and iron deposition in the kidney. Administration of DA markedly improved anemia to the normal control level and significantly alleviated DXR-induced increases of creatinine, blood urea nitrogen, renal interstitial fibrosis, renal iron deposition, and dry left ventricular weight, but serum and urinary iron and urinary protein and N-acetyl-β-*D*-glucosaminidase levels were unchanged. The urinary total radical-trapping antioxidant capacity was improved to the normal control level in DA-treated animals. DA reduced the DXR-induced cardiorenal injury. This improvement was achieved, when anemia was corrected to the normal control level.



## Introduction

In the United States, 20 million adults suffer from chronic kidney disease (CKD), and another 20 million are expected to face a heightened risk of developing CKD. An estimated 8 million adults have CKD of at least stage 3, distinguished by an estimated glomerular filtration rate <60 ml/min/1.73 $m^2$ [1]. Generally speaking, CKD is equivalent to progressive kidney disease towards end-stage renal disease; most patients suffer renal anemia because of insufficient erythropoietin production by the diseased kidney. Renal anemia provokes physiological abnormalities that are initially characterized by decreased oxygen delivery and utilization and increased cardiac output. These abnormalities are later characterized as left ventricular (LV) hypertrophy, decreased cognitive ability, and impaired immune response. Therefore, anemia of CKD should be treated during the predialysis period for improvement of patient survival [2] and quality of life [3]. Growing interest has centered upon the relation be-

KARGER
Fax +41 61 306 12 34
E-Mail karger@karger.ch
www.karger.com


1660–2129/06/1041–0006$23.50/0

Accessible online at:
www.karger.com/nee

Eisei Noiri, MD, PhD
Nephrology 107 Laboratory, Center for Dialysis, Apheresis, and Applied Medicine
University Hospital, University of Tokyo, 7-3-1 Hongo, Bunkyo
Tokyo 113-8655 (Japan)
Tel. +81 3 5800 8648, Fax +81 3 5818 3762, E-Mail noiri-tky@umin.ac.jp

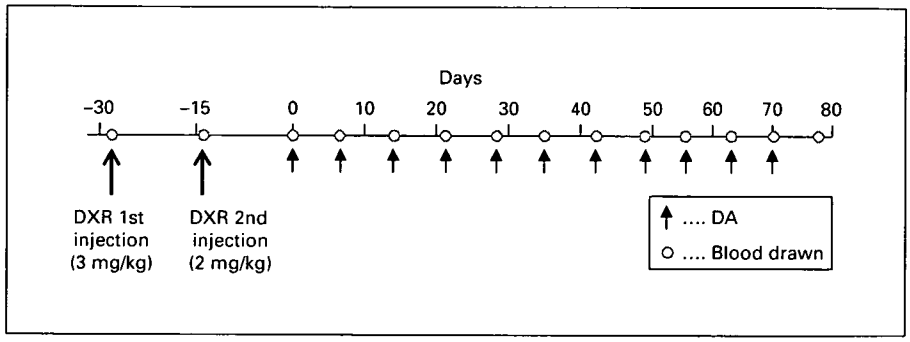


**Fig. 1.** Experimental protocol. Urine sampling was performed in a metabolic cage on days 71–72. The blood pressure was measured on days 75–76. Animals were sacrificed on days 77–78.

tween CKD and the risk of death, especially that caused by cardiovascular disease. Recent clinical studies [4–6] have suggested that mild-to-moderate elevations in serum creatinine (Cr) levels are associated with increased rates of death from cardiovascular causes.

Here, a question comes to our mind. If anemia in CKD is improved by erythropoietin administration, is it possible to reduce the histological deterioration in CKD and to improve renal outcome? If it were possible, then we might extend the diseased kidney's useful life span and delay initiation of dialysis therapy. Logically, we could then improve the cardiovascular outcome. Unfortunately, only limited data are available from chronic animal studies extrapolated to human CKD. Bahlmann et al. [7] clearly demonstrated the efficacy of long-acting erythropoietin, darbepoetin alfa (DA), in five-sixths-nephrectomized rats, in terms of renal tissue injury such as vascular endothelial injury, glomerular sclerosis, and tubular interstitial injury. However, renal anemia, which is common in CKD, did not develop at all in that study during the follow-up period. Bahlmann et al. [7] used a very low dose of DA (0.1 μg/kg) which did not affect hematocrit levels and did not warrant sufficient oxygen delivery to target organs.

Therefore, it is still questionable to improve the prognosis of CKD and end-stage renal disease at the clinical level. On the other hand, clinical erythropoietin therapy in CKD is intended to normalize renal anemia, but the rationale for that use to preserve other organs in addition to the kidney is still not sufficient.

For that reason, this study examined the efficacy of DA, a hyperglycosylated analog of recombinant human erythropoietin, in CKD accompanied by cardiovascular issues. We investigated doxorubicin hydrochloride (DXR) induced nephropathy in a rodent model of cardiorenal dysfunction syndrome, using either lower (3 μg/kg) or higher (30 μg/kg) doses of DA.

## Materials and Methods

*Materials*

The DXR used for this study was purchased from Kyowa Hakko Kogyo (Tokyo, Japan). DA was produced and supplied by Takasaki Pharmaceutical Plant (Kirin Brewery, Takasaki, Japan). All other chemicals were purchased from Wako Pure Chemical Industries (Osaka, Japan), unless otherwise specified. All rat experiments were approved by the Experimental Animal Ethical Committee of Kirin Brewery, in accordance with the NIH Guide for the Care and Use of Laboratory Animals [NIH Publication No. 86-23, 1985].

*Experimental Design*

The experimental protocol is shown in figure 1. Male 7-week-old Sprague-Dawley rats were purchased from Charles River Japan (Tokyo). They were allowed food and water ad libitum. All rats were kept in animal quarters with strictly controlled temperature (22 ± 3°C), humidity (55 ± 20%), and light conditions (lights on 08.00–20.00 h). After an acclimatization period of 11 days, the rats were assigned to the DXR group (n = 24) and the control group (n = 9); the protocol for the DXR group was performed according to our previously published report [8]. In the DXR group, the first injection of DXR at a dose of 3 mg/kg was performed 4 weeks and the second injection of DXR at a dose of 2 mg/kg 2 weeks before starting DA treatment. In the control group, the same volume (2 ml/kg) of saline was injected instead of DXR. Two different doses of DA (3 and 30 μg/kg s.c., once weekly) were used for the DXR group. Finally, 24 rats were assigned to DXR + vehicle (1 ml/kg), DXR + DA3 (3 μg/kg DA), and DXR + DA30 (30 μg/kg DA), each group consisting of 8 animals. Blood examinations were performed 4, 2, and 0 weeks before starting DA administration and subsequently 1, 2, 3, 4, 5, 6, 7, 8, 9, 10, and 11 weeks after starting DA administration. The rats were held separately in a metabolic cage to collect urine over 24 h, 71–72 days after starting DA administration. The blood pressure was monitored 75–76 days after starting DA administration. The animals were dissected 77–78 days after starting DA administration, and kidney specimens for pathological analyses were collected after vigorous perfusion with phosphate-buffered saline and were subsequently immersed in 10% buffered formalin. The left ventricle was carefully dissected out and analzed by weight after lyophilization.

*Peripheral Blood Counts*

Peripheral blood was drawn from the tail artery into EDTA-2K and used for the red blood cell (RBC) count and hemoglobin (Hb) concentration measurements using an automated analyzer (ADVIA 120 Hematology System; Bayer Medical, Tokyo).

*Blood Pressure*

The mean blood pressure in the conscious state was measured by the indirect tail cuff method using a model MK-2000 monitor for rats and mice (Muromachi Kikai, Tokyo), according to the manufacturer's instructions. The blood pressure was recorded as the mean value of three separate measurements obtained at each session.

*Blood Urea Nitrogen (BUN) and Cr*

The BUN was measured using a commercial kit (BUN II reagent kit; Wako Pure Chemical Industries). Serum and urinary Cr levels were measured by means of an enzymatic assay (CRE-EN; Kainos Laboratories, Tokyo), and the Cr clearance (CCr) was calculated from a standard formula.

*Urinary N-Acetyl-β-D-Glucosaminidase (NAG)*

NAG is an enzyme that is rich in renal tubular epithelial lysosomes. An increase of NAG is the hallmark of tubular epithelial cell injury. Absorbance at 580 nm measures the colorimetric reaction of *m*-cresol which is generated by the hydrolytic reaction of sodio-*m*-cresolsulfonphthaleinyl with NAG [9]. This assay was commercially available, and the entire process was conducted following the manufacturer's protocol (NAG test; Shionogi, Osaka).

*Serum and Urinary Iron Levels*

Serum and urinary iron measurements were performed after the release of iron from its binding proteins using thioglycolic acid; $Fe^{3+}$ was further reduced to $Fe^{2+}$ during this reaction. $Fe^{2+}$ reacting with 2-nitroso-5-(N-propyl-N-sulfopropylamino)-phenol generated a chelating complex that was detectable at a wavelength of 750 nm [10]. The assay kit was commercially available, and the entire process was conducted following the manufacturer's protocol (Fe C-test; Wako Pure Chemical Industries).

*Urinary Protein Excretion*

Urinary protein measurement was conducted during days 71–72 after starting the experiment. The urinary protein excretion was measured using a commercially available Micro TP kit (Wako Pure Chemical Industries).

*Urinary Evaluation for Total Radical-Trapping Antioxidant Capacity (TRAP)*

The renal antioxidant power under physiological or pathophysiological conditions consists of enzymatic and nonenzymatic antioxidative systems. Given the multiplicity of antioxidant pathways, the quantitative measurement of total antioxidant capacity will be the reasonable approach to evaluate a particular organ condition. For this purpose, the TRAP assay was performed for urine which predominantly reflects the renal antioxidant condition. In this assay, the reducing reaction of $Cu^{2+}$ to $Cu^{+}$ stably generates a 2:1 complex with the chromogen reagent and is measurable at approximately 490 nm using a plate reader. This colorimetric assay was used according to the manufacturer's protocol (TA 01; Oxford Biomedical Research, Oxford, Mich., USA).

*Histological Analysis*

The kidneys were embedded in paraffin (TissuePrep; Fisher Scientific, Pittsburgh, Pa., USA) and cut into 3-μm sections. After sequential dewaxing and rehydration, the sections were stained with periodic acid-Schiff, Masson's trichrome, and Berlin blue. Histological images were taken by means of a digital CCD camera (DXM 1200F; Nikon, Tokyo) and examined using an Optiphoto-2 microscope (Nikon).

*Morphological Evaluation of Kidneys*

The area of interstitial fibrosis in the cortex was evaluated with Masson's trichrome using a computer-aided evaluation program (AIS Ver4.0; Fujifilm, Tokyo). Under ×400 magnification, five randomly selected nonoverlapping fields from the cortical region were analyzed. The fibrotic areas that were stained in blue were picked up on digital images, and the percentage of the fibrotic area relative to the whole area of the field was calculated (% area). Glomeruli and large vessels were not included in the microscopic fields for image analyses. The scores of each kidney were averaged. The scores of respective animals were then averaged.

The iron deposition in Berlin blue staining was evaluated semiquantitatively in a blind fashion without prior knowledge of the rat group. At least ten fields were examined at ×400 in each specimen, and the iron staining of the lesion was graded from 0 to 4+, according to the percentage of Berlin blue staining. Consequently, a 1+ lesion represented an involvement of approximately 5% of the field, a 2+ lesion had involvement of 5–15%, a 3+ lesion indicated an involvement of 15–25%, and a 4+ lesion had an involvement >25% of the field. Each field represents 1.13 $mm^2$, resulting in a total explored area of 11.3 $mm^2$ in each kidney.

*Statistics*

The results are expressed as mean values ± SEM. Differences among experimental groups were determined using one-way ANOVA with Fisher's post hoc analysis. Differences with $p < 0.05$ were considered significant.

## Results

Both RBC and Hb values in the DXR group decreased significantly as compared with those of the DA-treated animals during the follow-up period (fig. 2). The level of anemia was normalized to that of the control group, when DA at 3 μg/kg was administered to DXR animals (DXR + DA3). The level of anemia was further improved in DXR animals that received 30 μg/kg of DA (DXR + DA30). The levels of RBC and Hb were significantly increased as compared with the control group. The time courses of BUN and Cr are summarized in figure 3. Both BUN and Cr levels increased gradually in the DXR group 6 weeks after starting DA administration. The levels of BUN and Cr in the DXR group were markedly reduced in the DA-treated animals. This improvement was not different for the animals treated with high and low doses of DA. Similarly, the CCr in the DXR group was signifi-

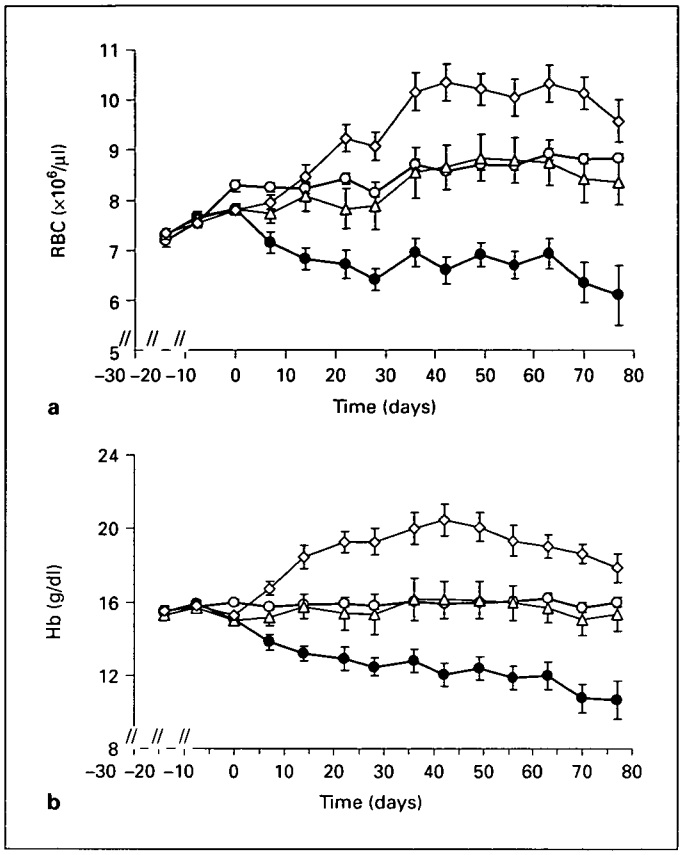


**Fig. 2.** Time courses of RBC (**a**) and Hb (**b**). ○ = Controls (n = 9); ● = DXR-treated animals (n = 8); △ = DXR + DA3 (low dose of DA; n = 8); ◇ = DXR + DA30 (high dose of DA; n = 8).

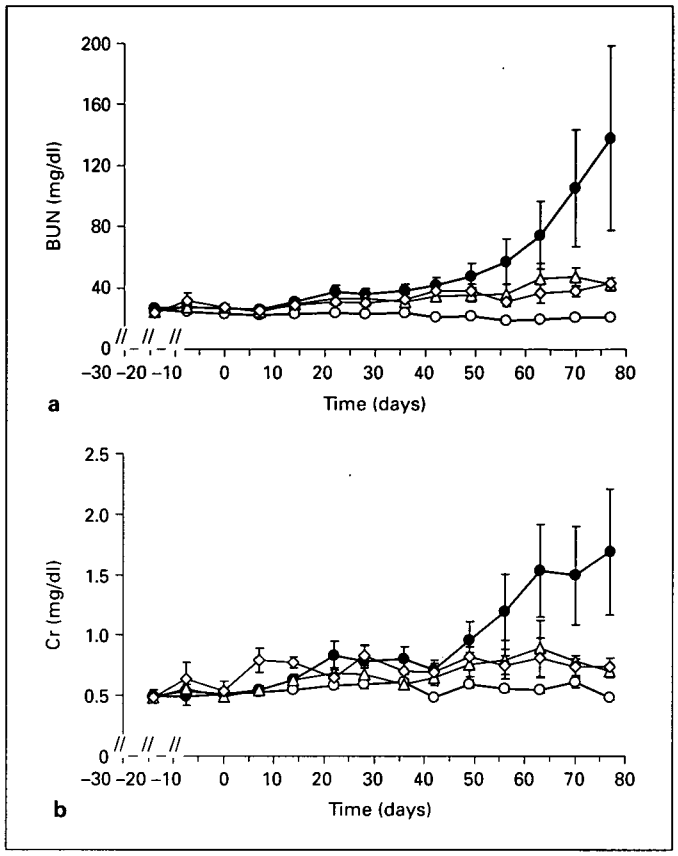


**Fig. 3.** Time courses of BUN (**a**) and Cr (**b**). ○ = Controls (n = 9); ● = DXR-treated animals (n = 8); △ = DXR + DA3 (low dose of DA; n = 8); ◇ = DXR + DA30 (high dose of DA; n = 8).

cantly decreased to 0.75 ± 0.22 ml/min as compared with the control group showing 2.15 ± 0.15 ml/min. This decrease in the CCr was improved in both animal groups treated with the low dose of DA (1.22 ± 0.10 ml/min) and with the higher dose of DA (1.32 ± 0.13 ml/min).

The mean blood pressure 75–76 days after starting the experimental protocols was 93.1 ± 8.8 mm Hg in the control group, 97.9 ± 12.4 mm Hg in the DXR group, 106.5 ± 9.3 mm Hg in the DXR + DA3 group, and 113.1 ± 8.6 mm Hg in the DXR + DA30 group. A tendency towards an increased mean blood pressure was apparent in the DA-treated groups, but this increase did not reach statistical significance.

Quantitative analysis of interstitial fibrosis was performed using Masson's trichrome staining. The severity of peritubular fibrosis was prominent in the kidneys of the DXR (DXR kidneys), as seen in figure 4a. The proportion of the fibrotic area (summarized in figure 4b) from the ×400 field was 36.43 ± 1.27% (n = 40 fields from eight kidneys) in the DXR kidneys as compared with 3.08 ± 0.34% (n = 45 fields from nine kidneys) in the control kidneys. This latter proportion was significantly lower for both doses of DA. The proportions of fibrotic areas were 7.59 ± 0.45% (n = 40 fields from eight kidneys) in the DXR + DA3 group and 7.51 ± 0.64% (n = 40 fields from eight kidneys) in the DXR + DA30 group. It is noteworthy that iron deposition represented by Berlin blue staining (fig. 5) was apparent in pericapillary interstitium and tubular basement membrane in the renal cortical region obtained from the DXR-treated animals. On the other hand, DA administration together with DXR reduced blue staining. Fine staining was, however, observed in proximal tubular cells in DXR kidneys treated with DA. Semiquantitative analyses indicated a significant increase of iron deposition in DXR animals. It was reduced to a statistically significant level in DA-treated kidneys in ani-

mals that received both the lower and the higher dosage ($p < 0.05$; fig. 5).

The serum iron level was decreased in the DXR group and in the DXR groups treated with with DA (DXR, 92.7 ± 10.9 μg/dl; DXR + DA3, 105.5 ± 11.0 μg/dl, DXR + DA30, 108.4 ± 15.8 μg/dl; n = 8 in each group) as compared with the control group (185.3 ± 5.1 μg/dl, n = 9) 77–78 days after starting DA administration. The urinary iron level was remarkably elevated in both the DXR group and the DXR groups treated with DA (DXR, 171.7

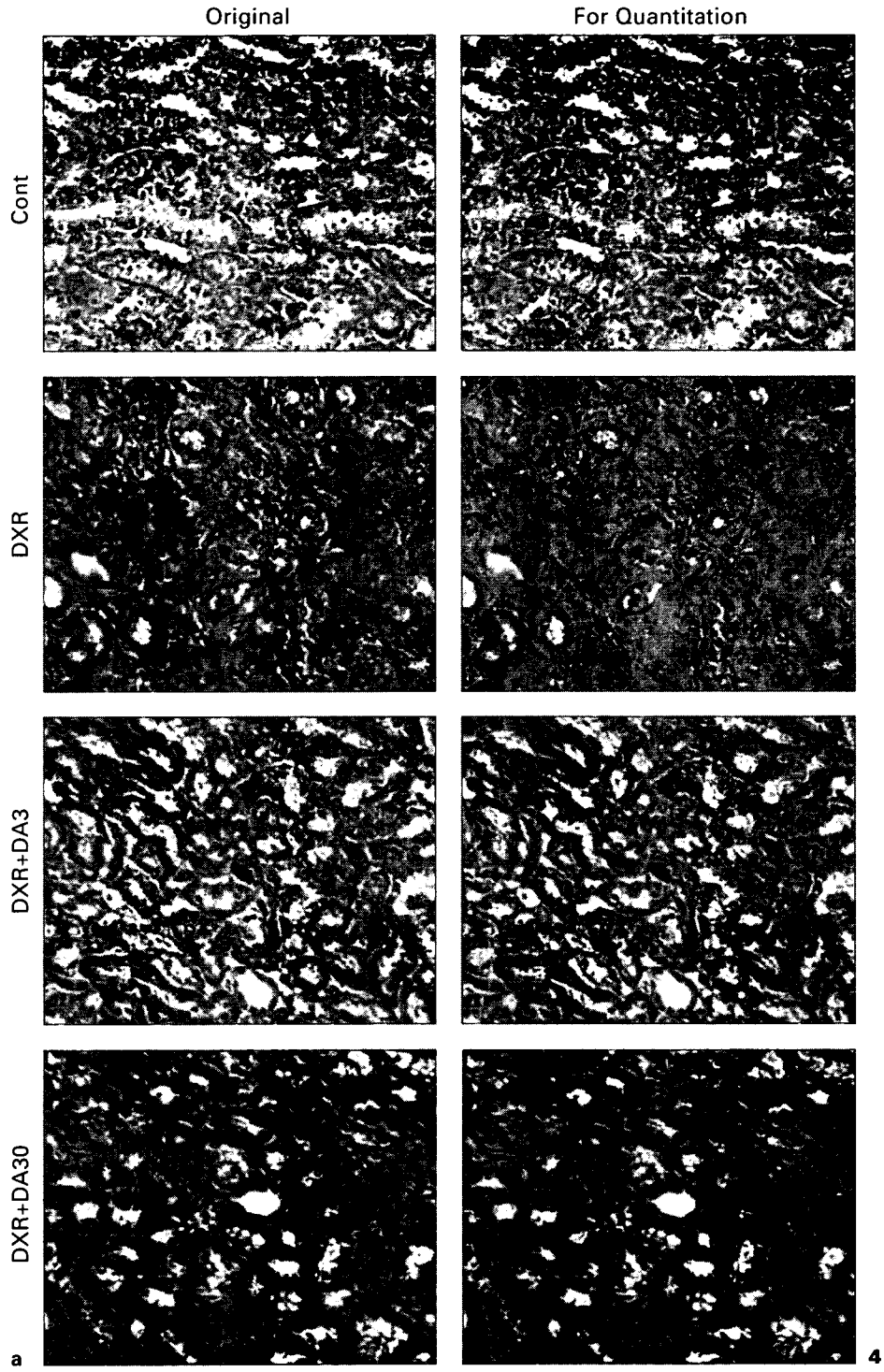


a 4

± 34.2 μg/kg; DXR + DA3, 214.8 ± 26.4 μg/kg; DXR + DA30, 223.5 ± 11.6 μg/kg) as compared with the control group (12.5 ± 1.8 μg/kg). The same phenomenon was found for the level of proteinuria (20.5 ± 1.8 μg/kg; DXR, 1,356.9 ± 192.4 μg/kg; DXR + DA3, 1,693.0 ± 214.0 μg/kg; DXR + DA30, 1,797.1 ± 159.6 μg/kg).

The level of urinary transferrin excretion is dependent on the level of proteinuria. Therefore, the ratio of urinary iron to proteinuria was calculated and is shown in figure 6. No significant difference was apparent between DXR groups with or without DA treatment. Therefore, the administration of DA per se did not promote iron excretion in this rodent CKD model.

The level of urinary NAG was significantly higher in the DXR-treated animals (2.96 ± 0.42 U/kg) than in the controls (0.78 ± 0.04 U/kg). No significant difference was apparent between DXR groups receiving DA (DXR + DA3, 3.05 ± 0.38 U/kg; DXR + DA30, 3.19 ± 0.49 U/kg).

The urinary measurement of TRAP (fig. 7) 71–72 days after starting DA administration revealed a significantly lower level in the DXR group (152.8 ± 18.2 μmol/kg) than in the control group (174.9 ± 16.7 μmol/kg). On the other hand, the TRAP level was significantly improved and even increased in the DXR-treated animals receiving both the lower DA dose (DXR + DA3, 214.0 ± 16.2 μmol/kg) and the higher DA dose (DXR + DA30, 240.2 ± 12.8 μmol/kg) as compared with the control or DXR-alone groups.

Finally, the index of the DXR-induced LV hypertrophy, represented as dry heart weight, is summarized in figure 8. The LV weight was significantly higher in the DXR group (592 ± 48 μg/kg; n = 8) as compared with

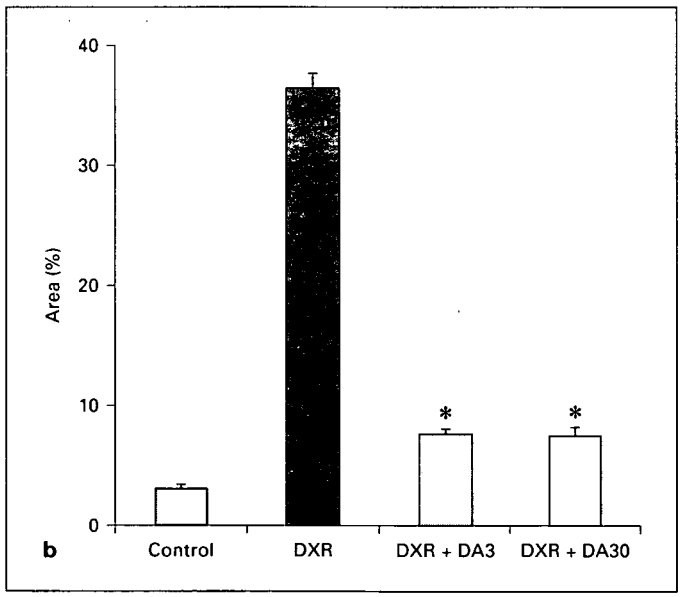


**Fig. 4. a** Representative images for renal interstitial quantitation. The level of blue color in Masson's trichrome staining (original) was gauged by image analysis software AIS and is expressed as light green in the right column. Glomeruli, tubular lumen, and large vessels were excluded from the microscopic fields. **b** The percentage of fibrotic areas relative to the whole area of the field was calculated. Asterisks indicate statistically significant difference when compared with the DXR-treated group ($p < 0.05$)

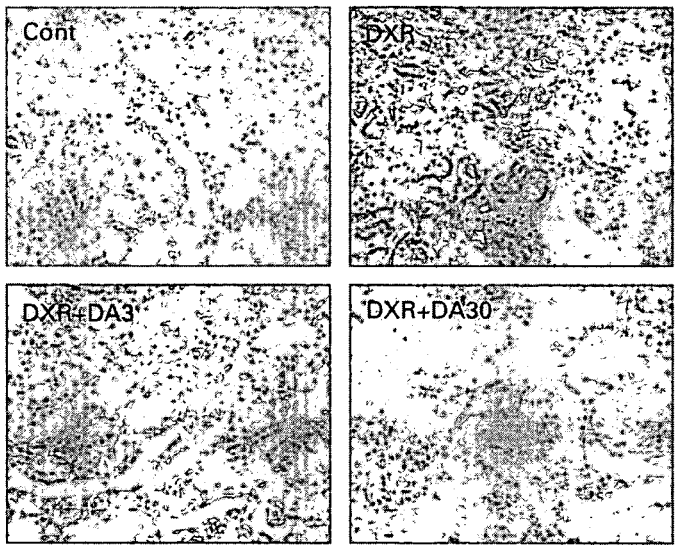


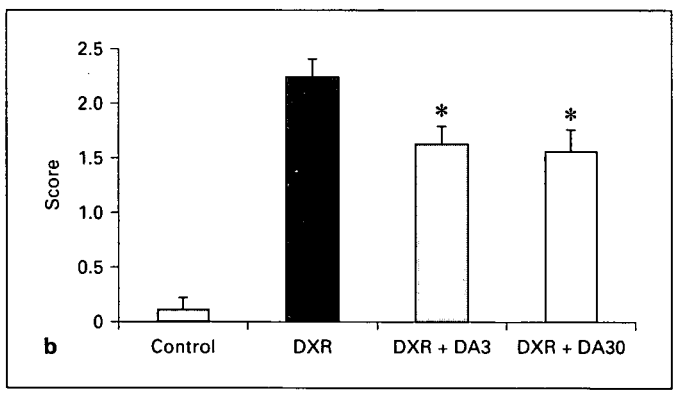


**Fig. 5.** Representative images of Berlin blue staining for iron deposition (**a**) and semi-quantitative analyses (**b**). Cont = Control. A 1+ lesion represented an involvement of approximately 5% of the field, a 2+ lesion an involvement of 5–15%, a 3+ lesion an involvement of 15–25%, and a 4+ lesion indicated involvement of more than 25% of the field. The asterisks in **b** indicate statistically significant difference when compared with the DXR-treated group ($p < 0.05$).

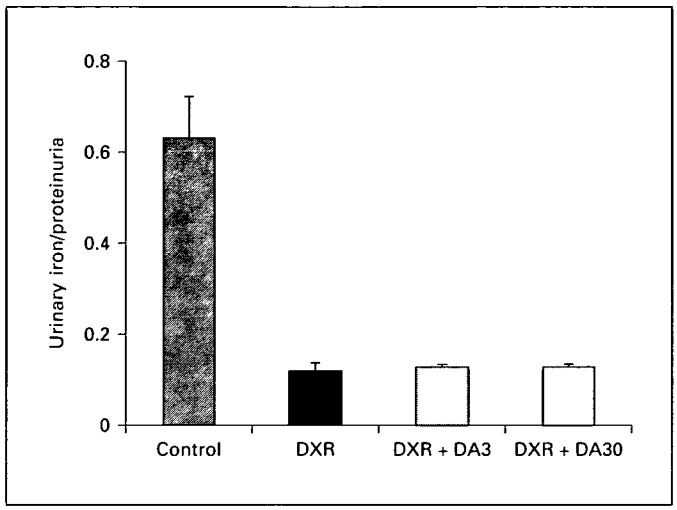


**Fig. 6.** Ratio of urinary iron excretion to proteinuria. Urine sampling was performed on days 71–72. The control group consisted of 9 animals, all others of 8 animals.

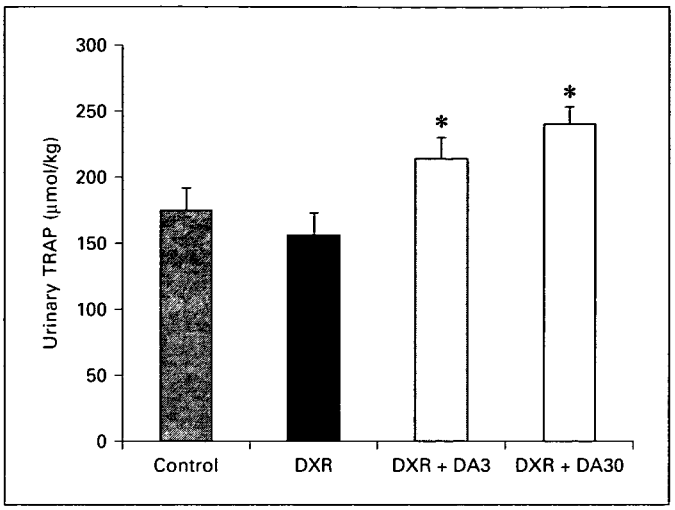


**Fig. 7.** Total urinary TRAP. Urine sampling was performed on days 71–72. The control group consisted of 9 animals, all others of 8 animals. Asterisks indicate statistically significant difference when compared with the DXR-treated group ($p < 0.05$).

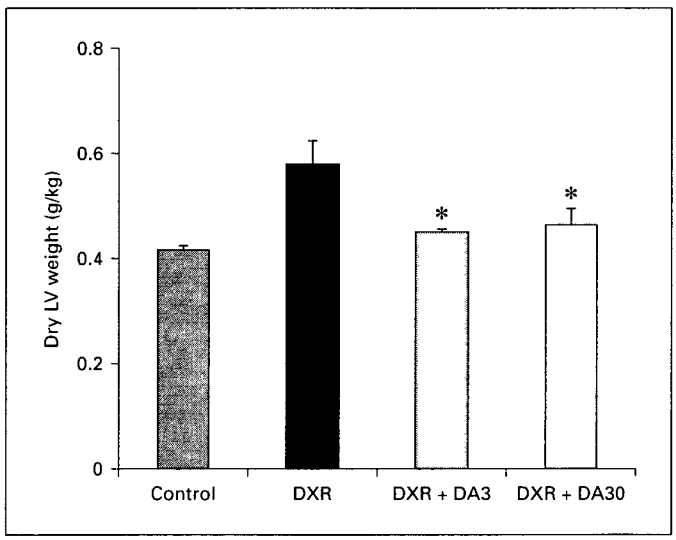


**Fig. 8.** Dry LV weight. The animals were dissected 77–78 days after starting DA administration. The control group consisted of 9 animals, all others of 8 animals. Asterisks indicate statistically significant difference when compared with the DXR-treated group ($p < 0.05$).

that of the control group (415 ± 8 µg/kg; n = 9). This increase was significantly ameliorated in the DA-treated animals receiving either the lower DA dose (DXR + DA3, 449 ± 7 µg/kg; n = 8) or the higher DA dose (DXR + DA30, 435 ± 9 µg/kg; n = 8).

## Discussion

The prevalence of anemia increases according to the stage of CKD, as addressed in recent K/DOQI guidelines [11]. Very few CKD individuals are anemic at stage III disease: about 15%. However, by stage IV, when the glomerular filtration rate is in the 15- to 29-ml/min/1.73 $m^2$ range, about 50% of the patients develop some degree of anemia. Several studies have reported that the level of the CCr is associated with adverse cardiovascular outcomes, particularly in patients with coronary artery disease [4, 6, 12–15]. In addition, a higher prevalence of renal insufficiency was reported in patients with heart failure. Multivariate analyses [16] of the RENAAL study [17] demonstrated that renal disease itself was an independent risk factor for developing cardiac disease just as hypertension, hyperlipidemia, smoking, and diabetes are. Furthermore, cardiac patients with anemia have worse outcomes; therapy of anemia improves their outcomes. If CKD, anemia, and cardiac disease share a triangular relationship, does treatment of anemia somehow forestall progression of CKD and cardiac disease? To answer this question, we have chosen DXR as a nephrotoxic and cardiotoxic agent in this study.

The DXR protocol used in this study clearly induced renal function deterioration, as demonstrated by BUN, Cr, and CCr. Correction of anemia to the level of the control group remarkably preserved renal functions; this

efficacy was equivalent for both the DXR group with a lower dose of DA and the DXR group with a higher dose of DA. The tubular injury marker NAG was not different between DXR-alone animals and DXR animals treated with lower or higher DA doses at days 71–72. Also, NAG did not reflect the differences observed in BUN, Cr, and CCr as a tubular injury marker in later stages of CKD. Histologically, the DXR kidneys showed tremendous fibrotic changes of the cortical tubular interstitium together with tubular atrophy and progressive scarring in the interstitium. These changes found in DXR kidneys were improved, when the animals were treated subsequently with either lower or higher doses of DA. These differences were quantitated using image analysis software to determine the statistically significant improvement of DA-treated kidneys over DXR kidneys. The dose of DA, either lower or higher, does not reflect this improvement. More intriguingly, DXR animals demonstrated more Berlin blue iron staining in their kidneys, especially at the cortical tubular basement, as shown in figure 5. This was reduced when DA was given to DXR animals. Next, we evaluated serum and urinary iron levels. The serum iron levels were reduced in all DXR animals, with or without DA treatment, probably due to urinary loss of transferrin together with proteinuria. No difference was apparent for the effect of DA on urinary iron levels in these animals. Therefore, the decrease of peritubular Berlin blue iron staining found in DA-treated DXR animals is presumably related to the increased hematopoiesis induced by DA which is, therefore, at least in part, able to decrease the level of tubular damage. This aspect was monitored by the urinary TRAP level. The TRAP level was rather more defective in DXR animals than in controls; it was significantly improved in DA-treated animals receiving either low or high doses. The improved findings observed in DA-treated kidneys were presumably related to chronic tubular rather than glomerular damage. These findings, therefore, support the concept that tubules and interstitium play a pivotal role in progressive kidney disease and are more predictive of the renal outcome. The oxygen tension of tubules is lower than that of glomeruli; tubules were more susceptible to hypoxic injury mediated by reactive oxygen species [18]. Treatment with erythropoietin will increase the oxygen delivery to these tissues, thereby reducing the risk of hypoxic injury.

DXR is a well-known cytotoxic drug causing cardiomyopathy, but the DXR dosage used in this study was far below that frequently used for the induction of DXR cardiomyopathy in rats [19]. Therefore, we believe that the factor related to diffuse cardiac fibrosis would be minimal in this study, but further histological studies are necessary. Anemia often promotes LV hypertrophy, and normalization of anemia by erythropoietin in predialysis CKD patients improved LV hypertrophy using the LV mass index as an indicator [20, 21]; this study elucidated this add-on effect. The LV dry weight, an alternative to the LV mass index in animal studies, was not increased in the present study, when the effect of anemia was improved in the DA groups receiving either low or high doses. These animal data further support results of a preceding human study reporting a 32% increased risk of a cardiovascular event for every 0.5-g/dl decrease in the Hb level in predialysis patients [22] and the finding that CKD patients with Hb levels <11.2 g/dl are three times more likely to progress to end-stage renal disease than those with Hb values >13.8 g/dl [16]. The observed efficacy of DA in DXR-induced LV hypertrophy will be partially derived from the direct effect of DA through erythropoietin receptors in cardiomyocytes, as seen in recent reports on rat ischemic heart models [23, 24], in addition to the indirect effect of DA: the increase of oxygen delivery to cardiomyocytes by correction of anemia. The erythropoietin-induced organ-protective effect against cardiorenal syndrome was achieved using a DA dose of 3 μg/kg which is sufficient to maintain a normal Hb level. The significant increase of the Hb levels beyond the normal control values was not important, because we were unable to detect further improvements in the parameters of our current study.

This animal study clarified the efficacy of DA in CKD and LV hypertrophy, supporting the clinical observations using erythropoietin reported by Gouva et al. [25]. In their report, patients who were treated with erythropoietin exhibited a dramatic increase in their Hb levels from 10 g/dl to almost 13 g/dl, whereas patients who were not treated showed no changes in Hb levels. Even though both groups had some decrease in their kidney function, this decrease was much more dramatic in patients that were not treated. Moreover, when these authors looked at their primary end points, doubling of serum Cr levels or progression to end-stage renal disease, patients who were not treated for their anemia had double the risk towards these end points. Based on these clinical data and the results of our study, correction of anemia to the normal level by erythropoietin or DA retards the progression of CKD and cardiovascular diseases.

## Acknowledgments

The first and the second author contributed equally to this study. Part of this study was supported by grants from the Araki Memorial Research Foundation (Tokyo, Japan; to E.N.), the Takeda Science Research Foundation (Osaka, Japan; to E.N.), the Foundation for Renal Anemia Therapy (Tokyo; to E.N.), and Health and Labour Science Research Grants for Research on Human Genome, Tissue Engineering, and Food Biotechnology from the Ministry of Health, Labour, and Welfare of Japan (to E.N.).

## References

1 Coresh J, Astor BC, Greene T, Eknoyan G, Levey AS: Prevalence of chronic kidney disease and decreased kidney function in the adult US population: Third National Health and Nutrition Examination Survey. Am J Kidney Dis 2003;41:1–12.
2 Collins AJ: Anaemia management prior to dialysis: cardiovascular and cost-benefit observations. Nephrol Dial Transplant 2003;18(Suppl 2):ii2–ii6.
3 Perlman RL, Finkelstein FO, Liu L, Roys E, Kiser M, Eisele G, Burrows-Hudson S, Messana JM, Levin N, Rajagopalan S, Port FK, Wolfe RA, Saran R: Quality of life in chronic kidney disease (CKD): a cross-sectional analysis in the Renal Research Institute-CKD study. Am J Kidney Dis 2005;45:658–666.
4 Mann JF, Gerstein HC, Pogue J, Bosch J, Yusuf S: Renal insufficiency as a predictor of cardiovascular outcomes and the impact of ramipril: the HOPE randomized trial. Ann Intern Med 2001;134:629–636.
5 Shlipak MG, Heidenreich PA, Noguchi H, Chertow GM, Browner WS, McClellan MB: Association of renal insufficiency with treatment and outcomes after myocardial infarction in elderly patients. Ann Intern Med 2002; 137:555–562.
6 Muntner P, He J, Hamm L, Loria C, Whelton PK: Renal insufficiency and subsequent death resulting from cardiovascular disease in the United States. J Am Soc Nephrol 2002;13: 745–753.
7 Bahlmann FH, Song R, Boehm SM, Mengel M, von Wasielewski R, Lindschau C, Kirsch T, de Groot K, Laudeley R, Niemczyk E, Guler F, Menne J, Haller H, Fliser D: Low-dose therapy with the long-acting erythropoietin analogue darbepoetin alpha persistently activates endothelial Akt and attenuates progressive organ failure. Circulation 2004;110:1006–1012.
8 Nagano N, Miyata S, Obana S, Ozai M, Kobayashi N, Fukushima N, Burke SK, Wada M: Sevelamer hydrochloride (Renagel), a non-calcaemic phosphate binder, arrests parathyroid gland hyperplasia in rats with progressive chronic renal insufficiency. Nephrol Dial Transplant 2001;16:1870–1878.
9 Le Hir M, Dubach UC, Guder WG: Distribution of acid hydrolases in the nephron of normal and diabetic rats. Int J Biochem 1980;12: 41–45.
10 Toei K, Motomizu S, Korenaga T: Nitrosophenol and nitrosonaphthol derivatives as reagents for the spectrophotometric determination of iron and determination of microamounts in waters with 2-nitroso-5-dimethylaminophenol. Analyst 1975;100:629–636.
11 National Kidney Foundation: K/DOQI clinical practice guidelines for chronic kidney disease: evaluation, classification, and stratification. Am J Kidney Dis 2002;39(suppl 1): S1–S266.
12 Manjunath G, Tighiouart H, Ibrahim H, MacLeod B, Salem DN, Griffith JL, Coresh J, Levey AS, Sarnak MJ: Level of kidney function as a risk factor for atherosclerotic cardiovascular outcomes in the community. J Am Coll Cardiol 2003;41:47–55.
13 Szczech LA, Best PJ, Crowley E, Brooks MM, Berger PB, Bittner V, Gersh BJ, Jones R, Califf RM, Ting HH, Whitlow PJ, Detre KM, Holmes D: Outcomes of patients with chronic renal insufficiency in the bypass angioplasty revascularization investigation. Circulation 2002;105:2253–2258.
14 Shlipak MG, Simon JA, Grady D, Lin F, Wenger NK, Furberg CD: Renal insufficiency and cardiovascular events in postmenopausal women with coronary heart disease. J Am Coll Cardiol 2001;38:705–711.
15 Culleton BF, Larson MG, Wilson PW, Evans JC, Parfrey PS, Levy D: Cardiovascular disease and mortality in a community-based cohort with mild renal insufficiency. Kidney Int 1999;56:2214–2219.
16 Keane WF, Brenner BM, de Zeeuw D, Grunfeld JP, McGill J, Mitch WE, Ribeiro AB, Shahinfar S, Simpson RL, Snapinn SM, Toto R: The risk of developing end-stage renal disease in patients with type 2 diabetes and nephropathy: the RENAAL study. Kidney Int 2003;63: 1499–1507.
17 Brenner BM, Cooper ME, de Zeeuw D, Keane WF, Mitch WE, Parving HH, Remuzzi G, Snapinn SM, Zhang Z, Shahinfar S; RENAAL Study Investigators: Effects of losartan on renal and cardiovascular outcomes in patients with type 2 diabetes and nephropathy. N Engl J Med 2001;345:861–869.
18 Rossert J, Fouqueray B, Boffa JJ: Anemia management and the delay of chronic renal failure progression. J Am Soc Nephrol 2003; 14(suppl 2):S173–S177.
19 Mettler FP, Young DM, Ward JM: Adriamycin-induced cardiotoxicity (cardiomyopathy and congestive heart failure) in rats. Cancer Res 1977;37:2705–2713.
20 Portoles J, Torralbo A, Martin P, Rodrigo J, Herrero JA, Barrientos A: Cardiovascular effects of recombinant human erythropoietin in predialysis patients. Am J Kidney Dis 1997;29: 541–548.
21 Hayashi T, Suzuki A, Shoji T, Togawa M, Okada N, Tsubakihara Y, Imai E, Hori M: Cardiovascular effect of normalizing the hematocrit level during erythropoietin therapy in predialysis patients with chronic renal failure. Am J Kidney Dis 2000;35:250–256.
22 Levin A, Thompson CR, Ethier J, Carlisle EJ, Tobe S, Mendelssohn D, Burgess E, Jindal K, Barrett B, Singer J, Djurdjev O: Left ventricular mass index increase in early renal disease: impact of decline in hemoglobin. Am J Kidney Dis 1999;34:125–134.
23 Calvillo L, Latini R, Kajstura J, Leri A, Anversa P, Ghezzi P, Salio M, Cerami A, Brines M: Recombinant human erythropoietin protects the myocardium from ischemia-reperfusion injury and promotes beneficial remodeling. Proc Natl Acad Sci USA 2003;100: 4802–4806.
24 Wright GL, Hanlon P, Amin K, Steenbergen C, Murphy E, Arcasoy MO: Erythropoietin receptor expression in adult rat cardiomyocytes is associated with an acute cardioprotective effect for recombinant erythropoietin during ischemia-reperfusion injury. FASEB J 2004; 18:1031–1033.
25 Gouva C, Nikolopoulos P, Ioannidis JP, Siamopoulos KC: Treating anemia early in renal failure patients slows the decline of renal function: a randomized controlled trial. Kidney Int 2004;66:753–760.

# Renal L-Type Fatty Acid–Binding Protein in Acute Ischemic Injury

Tokunori Yamamoto,* Eisei Noiri,† Yoshinari Ono,* Kent Doi,† Kousuke Negishi,† Atsuko Kamijo,‡ Kenjiro Kimura,‡ Toshiro Fujita,† Tsuneo Kinukawa,§ Hideki Taniguchi,‖ Kazuo Nakamura,¶ Momokazu Goto,* Naoshi Shinozaki,** Shinichi Ohshima,†† and Takeshi Sugaya‖**

*Department of Urology, University Hospital, Nagoya University, Nagoya, †Departments of Nephrology and Endocrinology, Hemodialysis and Apheresis, University Hospital, and Center of NanoBio Integration, University of Tokyo, Tokyo, ‡Department of Nephrology and Hypertension, St. Marianna University, Kawasaki, §Department of Urology, Chukyo Hospital, Nagoya, ‖Center for Developmental Biology, Riken, Kobe, ¶CMIC Co., Ltd., Tokyo, **Cornea Center, Tokyo Dental College Ichikawa General Hospital, Tokyo, and ††National Center for Geriatrics and Gerontology, Obu, Japan

## ABSTRACT

Fatty acid–binding proteins (FABPs) bind unsaturated fatty acids and lipid peroxidation products during tissue injury from hypoxia. We evaluated the potential role of L-type FABP (L-FABP) as a biomarker of renal ischemia in both human kidney transplant patients and animal models. Urinary L-FABP levels were measured in the first urine produced from 12 living-related kidney transplant patients immediately after reperfusion of their transplanted organs, and intravital video analysis of peritubular capillary blood flow was performed simultaneously. A significant direct correlation was found between urinary L-FABP level and both peritubular capillary blood flow and the ischemic time of the transplanted kidney (both $P < 0.0001$), as well as hospital stay ($P < 0.05$). In human-L-FABP transgenic mice subjected to ischemia-reperfusion injury, immunohistological analyses demonstrated the transition of L-FABP from the cytoplasm of proximal tubular cells to the tubular lumen. In addition, after injury, these transgenic mice demonstrated lower blood urea nitrogen levels and less histological injury than injured wild-type mice, likely due to a reduction of tissue hypoxia. *In vitro* experiments using a stable cell line of mouse proximal tubule cells transfected with h-L-FABP cDNA showed reduction of oxidative stress during hypoxia compared to untransfected cells. Taken together, these data show that increased urinary L-FABP after ischemic-reperfusion injury may find future use as a biomarker of acute ischemic injury.

*J Am Soc Nephrol* 18: 2894–2902, 2007. doi: 10.1681/ASN.2007010097

Mammalian intracellular fatty acid–binding proteins (FABP) are expressed from a large multigene family and encode 14-kD proteins that are members of the superfamily of lipid-binding proteins (LBP).[1] There are nine different FABP with tissue-specific distribution that include liver, intestinal, muscle and heart, adipocyte, epidermal, ileal, brain, myelin, and testis.[2] The epithelial FABP is unique among the LBP because of the presence of six cysteine residues, two of which, Cys-120 and -127, are modeled to form a disulfide bond within the ligand binding cavity. One report[3] showed that 4-hydroxynonenal (HNE), a cytotoxic $\alpha,\beta$-unsaturated acyl aldehyde produced from lipid peroxidation in response to oxidative stress, was able to modify the Cys-120 residue of E-FABP. Similarly, Wang *et al.*[4]

Received January 23, 2007. Accepted June 14, 2007.

Published online ahead of print. Publication date available at www.jasn.org.

**Correspondence:** Dr. Eisei Noiri, 107 Lab, Nephrology, University Hospital, University of Tokyo, 7-3-1 Hongo, Bunkyo, Tokyo, Japan 113-8655. Phone/Fax: 81-3-5814-8696; E-mail: noiri-1im@h.u-tokyo.ac.jp

demonstrated *in vitro* the potentiality of L-type FABP (L-FABP) to reduce oxidative stress in hypoxia-reoxygenation. When they increased the level of L-FABP expression, the intracellular oxidative stress was less. These studies, together with other studies,[5–7] have shown that FABP not only participate in fatty acid trafficking but also serve as early indicators of ischemic conditions and as important protective cellular antioxidant molecules that inactivate reactive lipids.

In the human kidney, L-FABP is expressed predominantly in the proximal tubules, a nephron segment that uses fatty acids as the major source of energy metabolism.[8] The role that L-FABP plays in ischemic injury has not been previously examined. Recent refinement of the previously described intravital video microscopy,[9] combined with sophisticated image analysis, has allowed us to monitor microcirculation in humans in a minimally invasive manner. In this study, we examined the role of L-FABP in ischemic conditions using the human model of kidney transplantation. This model is one of the most suitable models to evaluate a potential relationship between capillary blood flow and urinary parameters of acute kidney injury. Our results provide direct evidence that increased urinary levels of human L-FABP could represent an early biomarker of human renal ischemia. Furthermore, in concurrent studies using human L-FABP transgenic (h-L-FABP-Tg) mice, our results suggest that the expression of renal L-FABP protects kidney tissue from renal ischemic stress.

## RESULTS

Because the time point of clamping organ blood flow is definite in living-related human renal transplantation, it can be used to monitor a wide variety of pericapillary blood flow. Thus, living-related human renal transplantation provides an especially suitable model for examining the hemodynamics of peritubular capillary blood flow and urinary L-FABP. The actual ischemic time is determined easily and is monitored in each case. Twelve patients who had received living-related kidney transplantation were enrolled for capillary blood flow measurement. Intravital video charge-coupled device (CCD) images revealed a remarkable decrease of peritubular blood flow when measured close to the initiation of reperfusion. That flow gradually increased when measured at times further from reperfusion. The correlations between peritubular blood flow and the urinary markers defined already were examined and are shown in Figure 1. Among those markers, only urinary L-FABP correlated well to the increase of the reciprocal unit of peritubular capillary blood flow (1/blood flow; $n = 12$; $r = 0.933$, $P < 0.0001$); others did not reflect it. Urinary L-FABP becomes detectable when peritubular blood flow slows to <1 mm/s; consequently, the slower the peritubular blood flow, the higher the urinary L-FABP level.

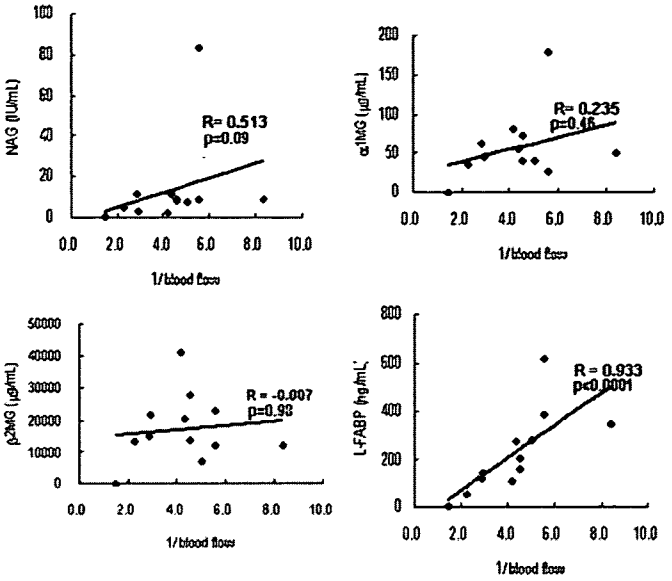


**Figure 1.** Correlation between peritubular capillary blood flow and urinary markers. Urinary markers are compared with 1/blood flow: Where renal ischemia is more severe, 1/blood flow is larger. Among the urinary markers examined, urinary L-FABP was most closely correlated with the decrease of peritubular blood flow.

We defined the ischemic time as the period between the time point of clamping the donor's renal artery and the time point of the appearance of virgin urine from the recipient's ureter. The urinary L-FABP values of that time point were collected, measured, and plotted together with ischemic time. As shown in Figure 2, urinary L-FABP and ischemic time showed an extremely significant correlation at the level of $r = 0.939$ ($n = 10$; $P < 0.0001$). All transplanted kidneys received renal biopsy 1 h after reperfusion—the so-called 1-h biopsy. Portions of 1-h biopsy specimens were examined immunohistochemically for L-FABP and compared with normal kidney. A representative image is shown in Figure 3. L-FABP was stained predominantly in the cytoplasmic region of normal human proximal tubules, as shown in the Figure 3, top (Normal). It is noteworthy that in ischemic kidney, the localization of L-FABP moved from the proximal tubular cells to the tubular lumen in

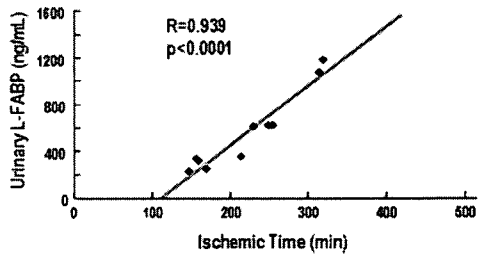


**Figure 2.** Correlation between ischemic time and urinary L-FABP. The ischemic time in living-related renal transplantation was defined as the period between the time point of clamping the donor's renal artery and the time point of appearance of virgin urine from the recipient's ureter. They showed an extremely significant correlation at the level of $r = 0.939$ ($n = 10$; $P < 0.0001$).

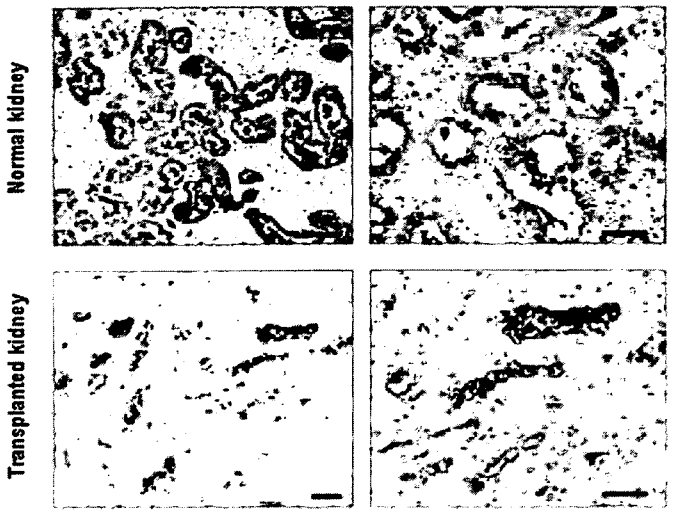


**Figure 3.** Immunohistochemical distribution of L-FABP. L-FABP was stained predominantly in the cytoplasmic region of the proximal tubule in intact human kidney (Normal kidney). It is noteworthy that the localization of L-FABP moved from the proximal tubular cells to the tubular lumen in a 1-h biopsy obtained from a patient with a successful medical record (Transplanted kidney), where the ischemic time was 4 h. The definition of ischemic time in this study was the period between the time point of clamping the donor's renal artery and the time point of appearance of virgin urine from the recipient's ureter. Bar = 50 $\mu$m. Magnifications: ×200 on left; ×400 on right.

a 1-h biopsy obtained from a patient who had a successful urine outcome 1 h after anastomosis in the transplant medical record (Figure 3, right). Because the postoperative renal function is virtually excellent in living-related renal transplantation, the improvement of renal function is very rapid. We observed that the pre- and postoperative levels of blood urea nitrogen (BUN) and serum creatinine (SCr) did not change significantly during the follow-up period. Urine N-acetyl-$\beta$-D-glucosaminidase (NAG) and $\beta$2-microglobulin levels also did not change during the follow-up period. No patient required renal replacement therapy after transplantation. The only finding obtained from those evaluations was the significant correlation between the hospital stay and urine L-FABP or renal microcirculation, where the correlation of the hospital stay with the initial urine L-FABP level of transplanted kidney was $r = 0.74$ ($n = 12$; $P < 0.05$). The correlation with renal microcirculation was $r = 0.89$ ($n = 12$; $P < 0.05$).

For further confirmation that urinary L-FABP is a biomarker reflecting proximal tubular ischemia, the human L-FABP gene with a 5′ promoter region was transferred to C57Bl/6 mice to obtain h-L-FABP-Tg mice. In these transgenic mice, it was confirmed that L-FABP was expressed predominantly in the proximal tubules, which was comparable to human kidney (Figure 3, Normal).

We next performed 30-min renal ischemia/reperfusion (I/R) injury in both h-L-FABP-Tg and wild-type mice. Blood was drawn sequentially from each mouse until 3 d after ischemia. Figure 4A shows the BUN profiles. The increase of BUN found 15 h after clamp release in the wild-type ischemic mice (110.1 ± 23.7 mg/dl [mean ± SD]; $n = 10$) was ameliorated in the ischemic h-L-FABP-Tg mice (75.0 ± 27.5; $n = 10$). Similarly, SCr increased from 0.22 ± 0.05 to 1.42 ± 0.2 mg/dl ($n = 10$) 15 h after I/R in the wild-type mice (Figure 4B). This increase was significantly ameliorated to a significant level in the ischemic h-L-FABP-Tg mice (1.12 ± 0.15 mg/dl; $n = 10$). The decrease in the ischemic h-L-FABP-Tg group continued at least 72 h after initiation of I/R. Histologic analyses were performed next. The representative histologic images of ischemic kidney 15 h after initiation of I/R are shown in Figure 5. An established protocol for quantification of histologic findings exists in renal I/R[10,11]; therefore, we followed this procedure of scoring for the evaluation, as reported previously.[12,13] Ischemic kidneys obtained from wild-type mice showed remarkable brush border loss, tubular dilation, tubular epithelial cell exfoliation, and widening of peritubular spaces. These findings

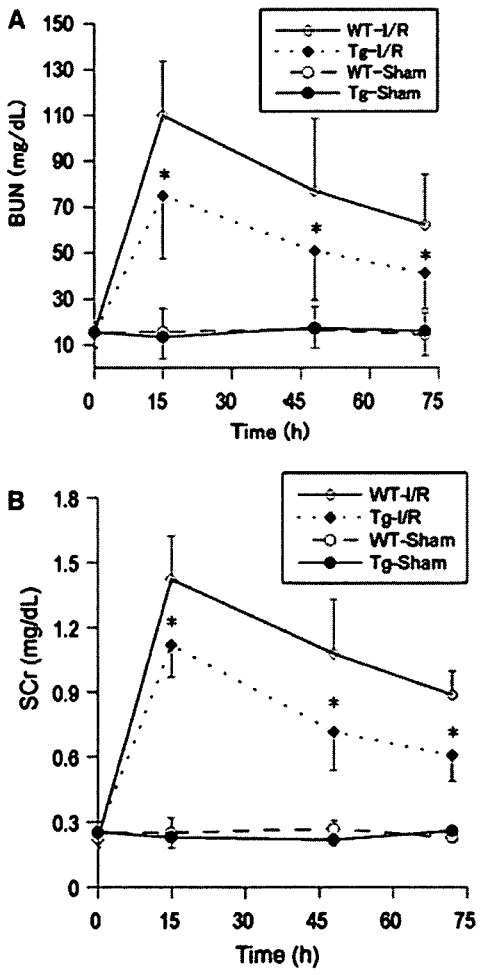


**Figure 4.** (A) Time course of BUN after renal I/R injury. (B) Time course of SCr after renal I/R injury. h-L-FABP-Tg I/R mice (Tg-I/R) showed half the level of BUN and SCr compared with that of wild-type (WT) I/R mice (WT-I/R) during all courses of experiments. This increase of BUN and SCr was ameliorated significantly in Tg-I/R ($n = 10$; $^*P < 0.05$).

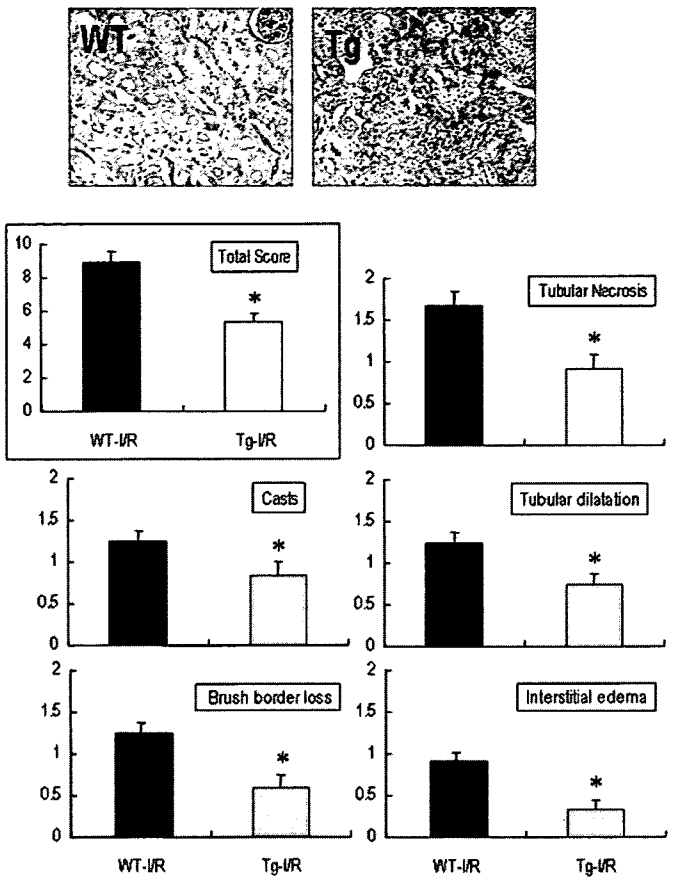


**Figure 5.** Representative histologies and acute tubular necrosis (ATN) score. Ischemic kidneys obtained from WT mice 15 h after initiation of I/R showed brush border loss, tubular dilation, tubular epithelial cell exfoliation, and widening of the peritubular space. These findings were markedly reduced in h-L-FABP-Tg mice. Each index and total score of those alleviated are shown quantitatively in bar graphs following the established protocol ($n = 10$; $^*P < 0.01$).

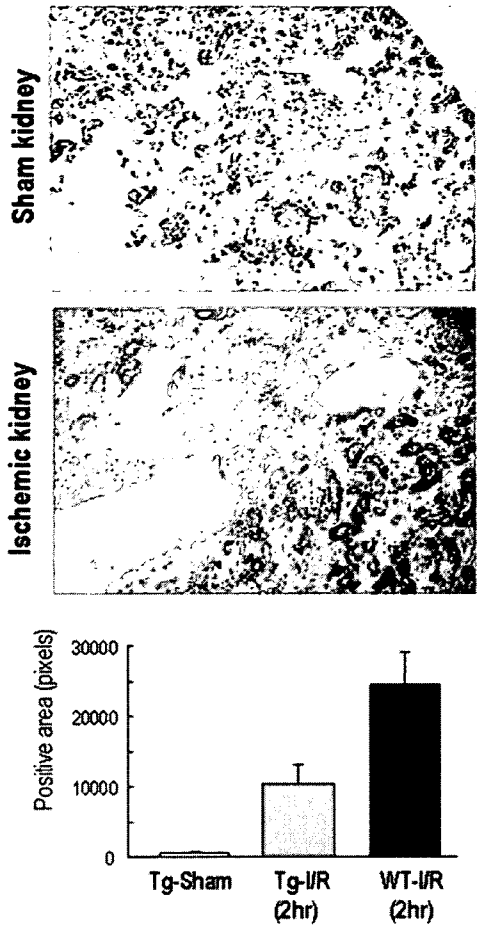


**Figure 6.** Renal distribution of L-FABP and hypoxia was examined in h-L-FABP-Tg mice subjected to renal I/R. The pimonidazole-positive hypoxic area (brown) expanded significantly in the outer medulla to the cortical region of ischemic h-L-FABP-Tg kidney. This area overlapped hardly at all with that of the L-FABP–positive proximal tubular cells (light green). The pimonidazole-positive hypoxic area was examined quantitatively using an image analysis platform, as summarized in the bar graph.

were significantly reduced in h-L-FABP-Tg kidneys, as shown in the bar graph of Figure 5. A statistically significant reduction was also found in the total scoring of all parameters in h-L-FABP-Tg kidneys.

Recently, it has become possible to demonstrate the hypoxic tissue condition using the hypoxic indicator pimonidazole that creates adducts during 1 to 2 h under oxygen tension of <10 mmHg. The specific antibody raised against this adduct is also commercially available. This system was applied to ischemic h-L-FABP-Tg mice to evaluate the localization of hypoxia and L-FABP. Figure 6, top, demonstrates the localization of both pimonidazole and L-FABP in sham-operated h-L-FABP-Tg kidneys. The L-FABP was clearly apparent in the proximal tubules in the outer medulla to the cortex, and staining of pimonidazole was not found in this group. In ischemic h-L-FABP-Tg kidney obtained 2 h after reperfusion, both pimonidazole and L-FABP were found in the proximal tubules of the outer medulla to the cortex (Figure 6, middle); however, those signals were not mutually overlapping. Hypoxic tubules did not express L-FABP any more at this time point, and/or tubules expressing L-FABP were not sufficiently hypoxic to the level to induce pimonidazole adduct formation. This observation suggests the potentiality that L-FABP is a molecule that preserves proximal tubules under hypoxia and that proximal tubules expressing L-FABP are presumably equivalent to vital tubules even in the ischemic renal condition.

The pimonidazole-positive area of ischemic kidney obtained 2 h after reperfusion was quantified using AIS (Fuji Photo Film, Tokyo, Japan). The pimonidazole-positive hypoxic area was expanded significantly in the outer medulla to the cortical region of ischemic h-L-FABP-Tg kidney compared with the sham-operated h-L-FABP-Tg kidney, whereas the hypoxic area seen in ischemic h-L-FABP-Tg kidney was considerably smaller than that of the ischemic wild-type kidney. Quantitative real-time PCR analyses were performed for kidneys harvested 8 and 24 h after I/R, and urinary L-FABP was

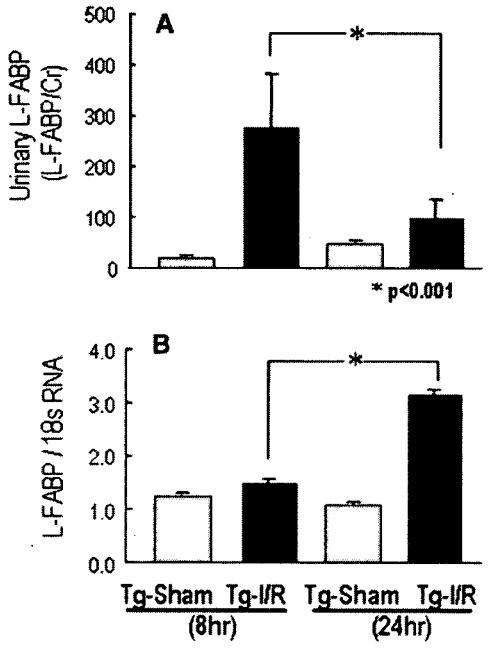


**Figure 7.** (A) Urinary L-FABP-to-Cr level in ischemic h-L-FABP-Tg mice. (B) Renal L-FABP transcriptional level in ischemic h-L-FABP-Tg mice. Both urine and renal tissue were obtained from the same mouse. A lag existed between urinary excretion of L-FABP and its renal transcription during I/R in h-L-FABP-Tg mice.

simultaneously monitored in the same mice. These combined results are shown in Figure 7. The transcription level of renal L-FABP increased significantly 24 h after reperfusion; that increase was not observed 8 h after I/R. Conversely, the urinary L-FABP level had increased by 8 h after reperfusion; this increase was alleviated 24 h after I/R. The effect of L-FABP on the hypoxic condition was examined *in vitro* with the comparison between mProx and mProx-L. The level of reactive oxygen species (ROS) was measured by CM-$H_2$DCFDA as previously reported,[13] and it was found that the level was remarkably reduced in mProx-L compared with mProx under hypoxia (Figure 8A, **). The transcription level in mProx-L cells was upregulated to the significant level under hypoxia (Figure 8B). In addition, the h-L-FABP level in the medium was significantly increased in that of hypoxic mProx-L compared with normoxia (Figure 8C).

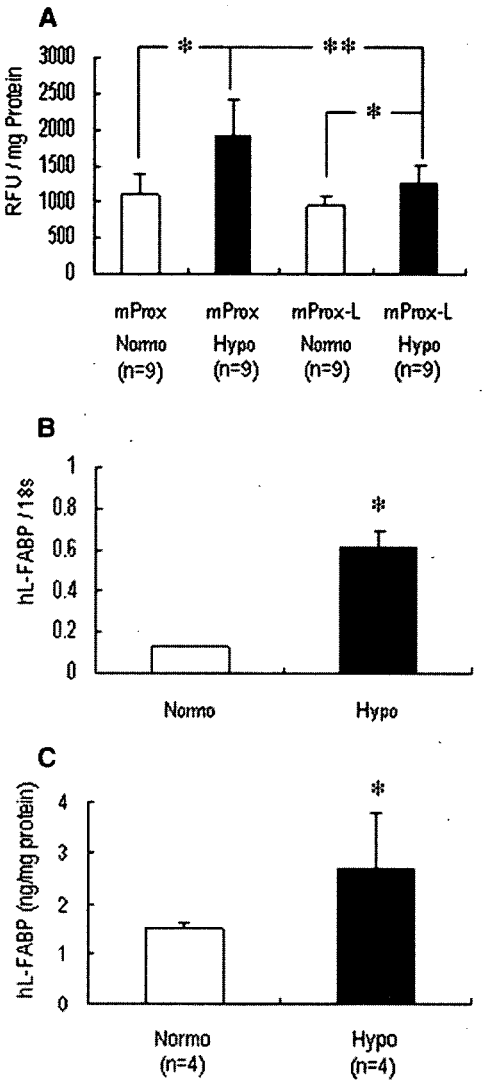


**Figure 8.** (A) Oxidative stress induced by hypoxia found in mProx was reduced in mProx-L to a significant level. Normo, normoxia; Hypo, hypoxia. The relative fluorescence unit (RFU) was normalized by the protein level. *$P < 0.01$. (B) The transcription level of human L-FABP was upregulated under hypoxia in mProx-L. Note that L-FABP was not expressed in mProx originally obtained from C57Bl/6 mice. Experiments were in quadruplicate. *$P < 0.05$, normoxia *versus* hypoxia; **$P < 0.05$ mProx *versus* mProx-L under hypoxia. (C) The protein level in cultured medium was compared between normoxia and hypoxia. Experiments were in quadruplicate. *$P < 0.05$.

## DISCUSSION

The FABP family comprises nine subtypes with organ-specific expression, some of which is linked closely to ischemic tissue conditions. Indeed, the I type of FABP, expressed in the small intestine, has been reported to increase in blood during the acute phase of intestinal artery thrombosis, a clinical condition that is difficult to diagnose in view of contemporary practical skill.[5] It is therefore expected to be the specific diagnostic marker of this disease. Moreover, in patients with acute myocardial infarction, it has been observed that the H type of FABP released from damaged or ischemic cardiac muscle appears in blood at the acute phase.[14] Recently, in comparison with the creatinine kinase MB-isoform or troponin-T, the blood concentration of H-type FABP was most sharply increased in patients visiting emergency departments for chest pain. Sandwich ELISA was found to be particularly useful for discovery of acute coronary syndrome within 6 h after its onset.[6]

In human kidney, L-FABP is expressed predominantly in proximal epithelial tubules, where FABP serves as a target of the highly cytotoxic aldehydes that are inevitably generated from lipid

peroxidation reaction during reperfusion; admittedly, FABP demonstrated its capability to bind with HNE, as demonstrated by Bennaars-Eiden *et al.*[3] The L-FABP presumably traps and transfers HNE to urinary spaces and sheds it into urine. Our study is the first to clarify the direct evidence of L-FABP localization in human proximal tubules with pericapillary blood flow. The translocation of L-FABP to urinary space under the ischemic condition was detectable by the ELISA method.

Given that L-FABP could act as a surrogate molecule that reduces lipid peroxidative stress in proximal tubular cells, the expression and upregulation of L-FABP *per se* might decrease renal ischemic insults. To answer that question, we produced h-L-FABP-Tg mice and subjected them to renal I/R. Tissue hypoxia after I/R was ameliorated remarkably in the presence of L-FABP, thereby demonstrating the orchestration among histologic hypoxia, L-FABP expression, and urinary L-FABP excretion. Admittedly, the reduction of oxidative stress under hypoxia was also more prominent in cells expressing human L-FABP *in vitro*. The upregulation of transcription level and increase of protein level were also confirmed *in vitro*. In addition, the chronological dynamics of the urinary L-FABP and cortical RNA level in h-L-FABP-Tg mice suggested a substantial feedback mechanism related to the promoter region of L-FABP controlling the renal proximal tubular L-FABP level.

It is noteworthy that L-FABP is not expressed in rodent kidney because nucleotides −4000 to −597, which are upstream of the rodents' L-FABP gene in their kidney, contain an orientation-independent suppressor sequence that prohibits renal expression.[15] In other words, rats and mice of wild type are equivalent to renal L-FABP–deficient animals, but renal expression of this molecule is secured in h-L-FABP-Tg mice; therefore, it is conceivable that the humanized kidneys are adopted in h-L-FABP-Tg mice in terms of this molecule. This might explain the discrepancy between findings in humans and rodents and the consequent criticism that the rodent model of acute renal failure, including the I/R model, does not correlate well with that in humans. That critique is related to the failure in clinical trials for acute renal failure that had been anticipated in light of favorable data of animal experiments.[16,17]

Using living-related renal transplantation, we observed the efficacy of urinary L-FABP as a biomarker of peritubular ischemia occurring after renal transplantation, and further found that the initial urine L-FABP level of transplanted kidney was the biomarker directly reflecting clinical outcome in terms of hospital stay. When the urine L-FABP level increased beyond 200 ng/ml, the duration of hospital stay became longer.

This finding was also confirmed in a murine renal I/R model using h-L-FABP-Tg mice. Further investigation is needed to evaluate the efficacy in cadaveric renal transplantation, vascular surgery that stops or reduces renal blood flow, catheter-related intervention that often accompanies renal arterial thromboembolization, and so forth. Urinary L-FABP is also promising for monitoring chronic ischemia, an essential mechanism for progressive chronic kidney disease (CKD). Kamijo *et al.*[18] investigated the urinary level in progressive CKD using a sandwich ELISA method for L-FABP. Their study concluded that the urinary level of L-FABP was the most sensitive indicator able to substantiate the prognosis of renal disease: Its use is superior to that of the SCr level, urinary protein level, or the urinary $\alpha$1-microglobulin level.[18] Other studies[19,20] emphasized chronic hypoxia in the tubulointerstitium as an alternative unifying mechanism of CKD progression. Chronic hypoxia in the kidney can occur according to structural changes that impair blood flow delivery to the tubules. In the event of glomerular sclerosis and/or interstitial fibrosis, the lesion is occupied by excessive extracellular matrix, which engenders the loss of microvasculature and renders both the lesion and its surrounding area hypoxic. That factor of chronic peritubular ischemia should also be considered as a mechanism of urinary L-FABP excretion in CKD. Furthermore, urinary L-FABP is now anticipated as a biomarker for type 2 diabetic nephropathy.[21]

On the basis of these data, the current hypothesis of L-FABP in renal proximal tubular epithelial cells is shown in Figure 9.

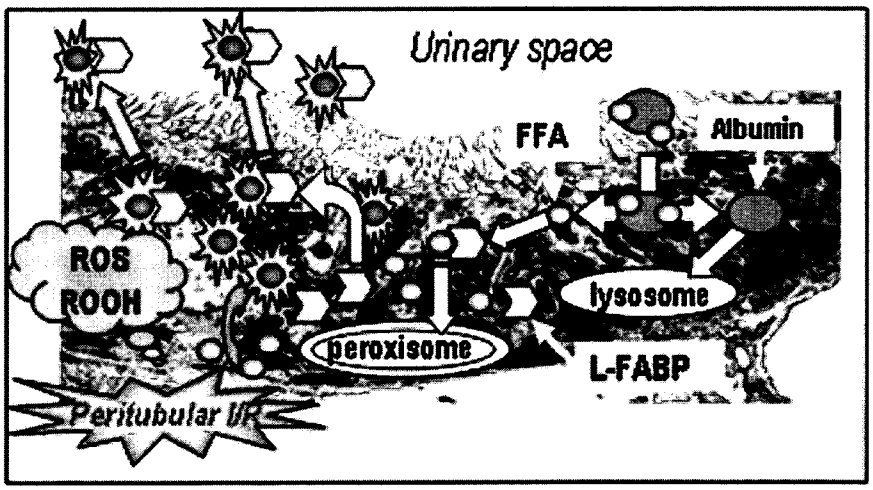


**Figure 9.** Conceptual schema for the renal L-FABP mechanism. In the kidney, albumin filtered from glomeruli is reabsorbed predominantly in proximal tubules together with free fatty acids (FFA) under physiologic conditions. After reabsorption, cytosolic albumin transfer to lysosome and fatty acid was released and received by L-FABP during this process. Fatty acid–bound L-FABP will usually be relocated to cytosolic peroxisome for size reduction of fatty acids. Under ischemic conditions, lipid peroxidation products will accumulate in proximal tubules and damage proximal tubules (left). L-FABP is presumably capable of binding these noxious lipid peroxidative products and transferring them to urinary spaces. L-FABP is excreted from the proximal tubules into urine by binding cytotoxic lipids. ROOH, hydroperoxide radicals.

Proximal tubular epithelial cells reabsorb >95% of urinary albumin that is filtered through a glomerular slit membrane. Free fatty acid bound to albumin is also incorporated into cellular cytoplasms together with albumin and is used for the β-oxidation–dependent tubular energy metabolic system. The L-FABP in proximal tubular epithelial cells serves as a shuttle of free fatty acid to appropriate cytosolic organella such as peroxisome, mitochondria, and/or extracellular urinary space (presumably a very small amount). In ischemic circumstances in human kidney, unsaturated fatty acids, the chemical characteristics of which are similar to that of detergents, are generated readily from cell membranes and cytoplasmic membranes. They are the major source of lipid-based peroxyradicals and aldehydes that are increased during I/R injury[13,22,23] and therefore propagate cellular injury *via* lipid peroxidation processes. The L-FABP molecule is capable of interrupting this reaction, especially binding fatty acids and aldehydes such as HNE into that pocket of β-sheet structure and relocating their distribution toward the tubular lumen, thereby preventing proximal tubular injury during ischemia and reperfusion.

Human L-FABP-Tg mice endowed with humanized kidneys, in contrast to those of wild-type rodents, are presumably more appropriate for the investigation of a renal disease model targeting human kidney disease. Especially in screening of newly discovered compounds for potential drugs, the h-L-FABP-Tg mouse model is better suited for nephrotoxicologic screening before going to clinical studies; therefore, it is more economical for future drug discovery processes. The characteristics of human L-FABP described here will fit the first and second topics of the Critical Path Opportunity List announced by the US Food and Drug Administration in 2006.

## CONCISE METHODS

### Protocol to Measure Peritubular Blood Flow and Urinary Markers of Proximal Tubule Injury in Living-Related Kidney Transplant Patients

During 12 living-related kidney transplant operations, peritubular capillary images were obtained using an intravital video CCD. The entire protocol of this study was explained to all patients, and their informed consent was obtained before initiation of the study, according to a protocol approved by the Human Study Committee of Nagoya University. Living-related kidney transplantation was performed using a method we reported previously.[24,25] Renal capillary blood flow was visualized and measured following the previously reported method with the adjustment for human renal capillary flow, as detailed in an online resource.[26] Urinary markers such as NAG, β2-microglobulin, and α1-microglobulin were monitored together with urinary L-FABP for comparison with peritubular capillary blood flow. Those markers except L-FABP were measured by the hospital's clinical pathology department. Urine collection was performed 24 h before transplantation from donors and subsequently performed after reperfusion of the transplanted kidney, where virgin urine and urine of indicated reperfusion time points were separately collected. Initiation of reperfusion is the time point that established anastomosis of the renal artery and vein of the transplanted kidney. Before anastomosis of the ureter, urine was collected directly from the ureter of the transplanted kidney.

### h-L-FABP-Tg Mice and the Renal I/R Model

The engineering of h-L-FABP-Tg mice is detailed elsewhere.[27] Briefly, genomic DNA of human L-FABP, including its promoter region (13 kb), was microinjected into fertilized eggs obtained from C57Bl/6 and CBA mice; ICR mice were used as transfected-egg recipients. The resultant transgenic mice were backcrossed for more than nine generations onto C57Bl/6 mice to obtain homozygous mutant mice with an inbred background. Only heterozygous h-L-FABP-Tg mice were used in this experiment. Male wild-type and h-L-FABP-Tg mice weighing 20 to 25 g were allowed food and water *ad libitum*. The mice were anesthetized using a combination of ketamine hydrochloride 11.6 mg/100 g and xylazine hydrochloride 0.77 mg/100 g and placed on a heated surgical pad. Rectal temperature was monitored using a sensitive thermistor for neonates (P1619; Nikkiso-YSI, Tokyo, Japan) with a data logger (600-1075; Barnant, Barrington, IL) and maintained 2°C above the initial core temperature. A 1.5-cm posterior lateral line incision was made, and both kidneys were exposed. Renal ischemia was initiated by clamping both renal arteries using microclips (Fine Science Tools, Foster City, CA). After 30 min, both clamps were removed; renal arteries were subsequently released. The incision was closed using a 3-0 suture and surgical staples. Mice were kept in glass-shielded metabolic cages (Metabolica; Sugiyamagen, Tokyo, Japan) until being killed, and urine was collected. Blood was drawn serially from each tail vein for BUN analyses 15, 48, and 72 h after surgery. Kidney specimens were collected 72 h after clamp release for immunohistochemistry and 2 h after injection of hypoxic probe. In a separate procedure, kidney specimens were collected 8 and 24 h for reverse transcriptase–PCR. All experiments were conducted in accordance with the National Institutes of Health Guide for the Care and Use of Laboratory Animals.

### Measurement of BUN and SCr

BUN and SCr were measured following the previously reported method.[28]

### Measurement of Urinary h-L-FABP by ELISA

Urinary h-L-FABP was measured by the sandwich ELISA kit following the manufacturer's protocol (CMIC, Tokyo, Japan). When intra-assay reproducibility was determined by the same sample eight times, the coefficient of variation for the obtained value was within 10%. The measurable range of this kit is between 4 and 400 ng/ml. The measurement was performed in duplication. The L-FABP value of healthy individuals including donor urine (before transplantation) was within the range of 0.12 to 20.09 ng/ml, and that mean is 1.60 ng/ml. In a part of the experiment, L-FABP was measured in cell culture medium. This assay system does not detect rodents' L-FABP, particularly that derived from wild type.

### Morphologic Evaluation of Kidneys

Formalin-fixed sections were stained with hematoxylin-eosin and periodic acid-Schiff. The morphologic evaluation of I/R injury was performed using well-established criteria in a blind manner.[10–13]

### Immunohistochemical Analyses

Immunohistochemical staining of 2-$\mu$m paraffin sections was performed using an indirect immunohistochemical technique. After deparaffinization, nonspecific reaction for horseradish peroxidase was blocked by 3% hydrogen peroxide in methyl alcohol for 10 min. Human specimens were subsequently blocked by goat serum (Dako-Japan, Kyoto, Japan). Mice specimens were blocked initially by Blocking A solution of Histofine Mice Stain Kit (Nichirei, Tokyo, Japan) for mouse tissue immunohistochemical staining using mouse mAb. A primary mAb (CMIC) against h-L-FABP (not cross-reacting to mice L-FABP) of 1:500 dilutions was applied to sections and incubated for 1 h at room temperature. The subsequent procedure of mouse sections was conducted according to the manufacturer's instructions of the Histofine Mice Stain Kit. That of human sections was followed by Vectastain ABC system (Vector Laboratories, Burlingame, CA) protocol. For substrate-chromogen reaction, diaminobenzidine tetrahydrochloride (Simple Stain DAB; Nichirei) was used following the manufacturer's protocol. Control sections were subjected to secondary antibody only (blank). Mounted preparations were examined using light microscopy (Nikon Eclipse 80i; Nikon, Tokyo, Japan). Images were captured by CCD camera (DXM1200F; Nikon).

### Experiment with Hypoxic Probe

The level of the outer medulla to cortical ischemia was evaluated immunohistochemically using a hypoxic probe-1 system of pimonidazole (Chemicon, Temecula, CA). Pimonidazole was injected into mice *via* a tail vein 1 h before starting ischemia. After 30 min of ischemia, another 2 h was used for the reperfusion period. During this 2-h period, pimonidazole was reductively activated and protein adducts were generated. The specific antibody (Chemicon) raised against this particular adduct was used for detection of the hypoxic area. Mice were then killed, and their kidneys were fixed into 10% buffered formalin. Immunohistochemistry was performed following the manufacturer's protocol. For evaluation of pimonidazole, the positive area and expression of h-L-FABP in ischemic h-L-FABP-Tg kidney, staining obtained from serial sectioning, were combined using the overlay function of image software (MetaMorph 5.0; Universal Imaging, Downingtown, PA); simultaneously, the hypoxic area and L-FABP–positive area were quantified using another image software package (AIS).

### Real-Time Quantitative PCR Analysis

Total RNA was extracted from the outer medulla to cortical kidney homogenates using Trizol (Invitrogen, Carlsbad, CA). In a part of the experiment, total RNA was extracted from cultured cells. To synthesize cDNA from total RNA, we used SuperScript II Reverse Transcriptase (Invitrogen). Renal mRNA levels were assessed using real-time quantitative PCR with TaqMan Universal PCR Master Mix (Applied Biosystems, Foster City, CA) and a Prism 7000 PCR system (Applied Biosystems) according to the manufacturer's instructions. Each gene and PCR primer was obtained from Assay-on-Demand (Applied Biosystems) as follows: h-L-FABP, assay ID Hs00155026_m1; and 18s ribosomal RNA, assay ID Hs99999901_s1.

### Fluorescence Measurement of Intracellular ROS

The stable C57Bl/6 mice proximal tubular cell line, mProx, was obtained by the previously reported method without virus transfection.[29] Because mProx does not express L-FABP, h-L-FABP including the promoter region was transfected to mProx by FuGene 6 (Roche, Mannheim, Germany) and mProx-L was obtained. As seen in Figure 8B, mProx is stably expressing h-L-FABP. Both mProx and mProx-L were maintained by K-1 medium supplemented with ITS (BD Pharmingen, San Diego, CA), $10^{-8}$ M dexamethasone, 2.5 mM nicotinamide, and 10% FBS (JRH Biosciences, Lenexa, KS). Both cells were lifted with 0.05% trypsin-0.53 mM EDTA (Invitrogen) and washed, and $1.5 \times 10^4$ cells/ml suspended in 200 $\mu$l of that culture medium were seeded per well in 96-well plates (Corning, Corning, NY) in a part of the experiment. To measure intracellular ROS production, both mProx and mProx-L were changed to serum reduced (0.5% FBS) experimental medium. Both mProx and mProx-L were subjected to hypoxia for 24 h using BBL GasPak Pouch (BD Pharmingen). Cells were loaded with 10 $\mu$M CM-$H_2$DCFDA (Invitrogen) for 30 min at 37°C in the dark following the previously reported protocol.[13] During each experiment, fluorescence of CM-$H_2$DCFDA was measured on four separate cell monolayers using an excitation wavelength of 485 nm and an emission wavelength of 538 nm by a fluorescence microplate reader (fMax; Molecular Devices, Sunnyvale, CA). Nine samples were prepared for each group.

### Evaluation of Clinical Outcome

To evaluate the clinical outcome in each of the 12 patients studied, we compared the parameters of the urine drained from the transplanted kidney ureter (*i.e.*, initial levels of L-FABP, NAG, and $\beta$2-microglobulin) and renal microcirculation of the transplanted kidney with the representative parameters reflecting clinical outcome, as follows: Levels of postoperative BUN and SCr, occurrence of renal replacement therapy after transplantation, and duration of hospital stay.

### Statistical Analyses

Correlations between two indicators were evaluated using Spearman rank test, and $r > 0.6$ was considered a significant correlation. Differences among experimental groups were detected by one-way ANOVA using Scheffe *post hoc* analysis. Values are expressed as means ± SD; $P < 0.05$ was considered significant. Statistical analysis was performed by SAS 9.1 (SAS Institute Japan, Tokyo, Japan).

## ACKNOWLEDGMENTS

Part of this study was supported by the Health and Labor Sciences Research Grants for Research on Human Genome, Tissue Engineering Food Biotechnology, MHLW, Japan (057100000661 to T.Y., E.N., Y.O., H.T., N.S., S.O., and T.S.); by the BioBank Japan Project on the Implementation of Personalized Medicine, MEXT, Japan (3023168 to E.N.); by Special Coordination Funds for Promoting Science and

Technologies, MEXT, Japan (1200015 to E.N.); and by KAKENHI, MEXT, Japan (19590935 to E.N. and T.S.).

We are grateful to Ms. Yokura, Mr. Okamoto, Dr. Fujita, Dr. Tsuji, and Ms. Maeda for skilled assistance.

## DISCLOSURES

None.

## REFERENCES

1. Tan NS, Shaw NS, Vinckenbosch N, Liu P, Yasmin R, Desvergne B, Wahli W, Noy N: Selective cooperation between fatty acid binding proteins and peroxisome proliferator-activated receptors in regulating transcription. *Mol Cell Biol* 22: 5114–5127, 2002
2. Chmurzynska A: The multigene family of fatty acid-binding proteins (FABPs): Function, structure and polymorphism. *J Appl Genet* 47: 39–48, 2006
3. Bennaars-Eiden A, Higgins L, Hertzel AV, Kapphahn RJ, Ferrington DA, Bernlohr DA: Covalent modification of epithelial fatty acid-binding protein by 4-hydroxynonenal in vitro and in vivo: Evidence for a role in antioxidant biology. *J Biol Chem* 277: 50693–50702, 2002
4. Wang G, Gong Y, Anderson J, Sun D, Minuk G, Roberts MS, Burczynski FJ: Antioxidative function of L-FABP in L-FABP stably transfected Chang liver cells. *Hepatology* 42: 871–879, 2005
5. Kanda T, Fujii H, Fujita M, Sakai Y, Ono T, Hatakeyama K: Intestinal fatty acid binding protein is available for diagnosis of intestinal ischaemia: Immunochemical analysis of two patients with ischaemic intestinal diseases. *Gut* 36: 788–791, 1995
6. Nakata T, Hashimoto A, Hase M, Tsuchihashi K, Shimamoto K: Human heart-type fatty acid-binding protein as an early diagnostic and prognostic marker in acute coronary syndrome. *Cardiology* 99: 96–104, 2003
7. Kamijo-Ikemori A, Sugaya T, Obama A, Hiroi J, Miura H, Watanabe M, Kumai T, Ohtani-Kaneko R, Hirata K, Kimura K: Liver-type fatty acid-binding protein attenuates renal injury induced by unilateral ureteral obstruction. *Am J Pathol* 169: 1107–1117, 2006
8. Portilla D: Energy metabolism and cytotoxicity. *Semin Nephrol* 23: 432–438, 2003
9. Yamamoto T, Tada T, Brodsky SV, Tanaka H, Noiri E, Kajiya F, Goligorsky MS: Intravital videomicroscopy of peritubular capillaries in renal ischemia. *Am J Physiol Renal Physiol* 282: F1150–F1155, 2002
10. Conger JD, Schultz MF, Miller F, Robinette JB: Responses to hemorrhagic arterial pressure reduction in different ischemic renal failure models. *Kidney Int* 46: 318–323, 1994
11. Solez K, Morel-Maroger L, Sraer JD: The morphology of "acute tubular necrosis" in man: Analysis of 57 renal biopsies and a comparison with the glycerol model. *Medicine (Baltimore)* 58: 362–376, 1979
12. Noiri E, Peresleni T, Miller F, Goligorsky MS: In vivo targeting of inducible NO synthase with oligodeoxynucleotides protects rat kidney against ischemia. *J Clin Invest* 97: 2377–2383, 1996
13. Doi K, Suzuki Y, Nakao A, Fujita T, Noiri E: Radical scavenger edaravone developed for clinical use ameliorates ischemia/reperfusion injury in rat kidney. *Kidney Int* 65: 1714–1723, 2004
14. Van Nieuwenhoven FA, Kleine AH, Wodzig WH, Hermens WT, Kragten HA, Maessen JG, Punt CD, Van Dieijen MP, Van der Vusse GJ, Glatz JF: Discrimination between myocardial and skeletal muscle injury by assessment of the plasma ratio of myoglobin over fatty acid-binding protein. *Circulation* 92: 2848–2854, 1995
15. Simon TC, Roth KA, Gordon JI: Use of transgenic mice to map cis-acting elements in the liver fatty acid-binding protein gene (Fabpl) that regulate its cell lineage-specific, differentiation-dependent, and spatial patterns of expression in the gut epithelium and in the liver acinus. *J Biol Chem* 268: 18345–18358, 1993
16. Allgren RL, Marbury TC, Rahman SN, Weisberg LS, Fenves AZ, Lafayette RA, Sweet RM, Genter FC, Kurnik BR, Conger JD, Sayegh MH: Anaritide in acute tubular necrosis. Auriculin Anaritide Acute Renal Failure Study Group. *N Engl J Med* 336: 828–834, 1997
17. Wang S, Hirschberg R: Role of growth factors in acute renal failure. *Nephrol Dial Transplant* 12: 1560–1563, 1997
18. Kamijo A, Kimura K, Sugaya T, Yamanouchi M, Hikawa A, Hirano N, Hirata Y, Goto A, Omata M: Urinary fatty acid-binding protein as a new clinical marker of the progression of chronic renal disease. *J Lab Clin Med* 143: 23–30, 2004
19. Fine LG, Bandyopadhay D, Norman JT: Is there a common mechanism for the progression of different types of renal diseases other than proteinuria? Towards the unifying theme of chronic hypoxia. *Kidney Int Suppl* 75: S22–S26, 2000
20. Kang DH, Kanellis J, Hugo C, Truong L, Anderson S, Kerjaschki D, Schreiner GF, Johnson RJ: Role of the microvascular endothelium in progressive renal disease. *J Am Soc Nephrol* 13: 806–816, 2002
21. Noiri E, Tsukahara H: Parameters for measurement of oxidative stress in diabetes mellitus: Applicability of enzyme-linked immunosorbent assay for clinical evaluation. *J Investig Med* 53: 167–175, 2005
22. Paller MS, Hoidal JR, Ferris TF: Oxygen free radicals in ischemic acute renal failure in the rat. *J Clin Invest* 74: 1156–1164, 1984
23. Noiri E, Nakao A, Uchida K, Tsukahara H, Ohno M, Fujita T, Brodsky S, Goligorsky MS: Oxidative and nitrosative stress in acute renal ischemia. *Am J Physiol Renal Physiol* 281: F948–F957, 2001
24. Takeuchi N, Ohshima S, Ono Y, Sahashi M, Matsuura O, Yamada S, Tanaka K, Kuriki O, Kamihira O: Five-year results of thoracic duct drainage in living related donor kidney transplantation. *Transplant Proc* 24: 1421–1423, 1992
25. Hashimoto Y, Nagano S, Ohsima S, Takahara S, Fujita T, Ono Y, Kinukawa T: Surgical complications in kidney transplantation: Experience from 1200 transplants performed over 20 years at six hospitals in central Japan. *Transplant Proc* 28: 1465–1467, 1996
26. Yamamoto T, Kajiya F: Intravital videomicroscopy. *Methods Mol Med* 86: 119–128, 2003
27. Kamijo A, Sugaya T, Hikawa A, Okada M, Okumura F, Yamanouchi M, Honda A, Okabe M, Fujino T, Hirata Y, Omata M, Kaneko R, Fujii H, Fukamizu A, Kimura K: Urinary excretion of fatty acid-binding protein reflects stress overload on the proximal tubules. *Am J Pathol* 165: 1243–1255, 2004
28. Doi K, Okamoto K, Negishi K, Suzuki Y, Nakao A, Fujita T, Toda A, Yokomizo T, Kita Y, Kihara Y, Ishii S, Shimizu T, Noiri E: Attenuation of folic acid-induced renal inflammatory injury in platelet-activating factor receptor-deficient mice. *Am J Pathol* 168: 1413–1424, 2006
29. Okada H, Kikuta T, Inoue T, Kanno Y, Ban S, Sugaya T, Takigawa M, Suzuki H: Dexamethasone induces connective tissue growth factor expression in renal tubular epithelial cells in a mouse strain-specific manner. *Am J Pathol* 168: 737–747, 2006

Supplemental information for this article is available online at http://www.jasn.org/.